USGS
science for a changing world

Groundwater and Streamflow Information Program

Dynamic Rating Method for Computing Discharge from Time-Series Stage Data

Open-File Report 2022–1031

U.S. Department of the Interior
U.S. Geological Survey

Dynamic Rating Method for Computing Discharge from Time-Series Stage Data

By Marian Domanski, Robert R. Holmes, Jr., and Elizabeth N. Heal

Groundwater and Streamflow Information Program

Open-File Report 2022–1031

U.S. Geological Survey, Reston, Virginia: 2022

For more information on the USGS—the Federal source for science about the Earth, its natural and living resources, natural hazards, and the environment—visit https://www.usgs.gov or call 1–888–ASK–USGS.

For an overview of USGS information products, including maps, imagery, and publications, visit https://store.usgs.gov/.

Suggested citation:
Domanski, M., Holmes, R.R., Jr., and Heal, E.N., 2022, Dynamic rating method for computing discharge from time-series stage data: U.S. Geological Survey Open-File Report 2022–1031, 48 p., https://doi.org/10.3133/ofr20221031.

Associated data:
Domanski, M.M., Holmes, R.R., and Heal, E.N., 2022a, Dynamic rating method for computing discharge from time series stage data—Site datasets: U.S. Geological Survey data release, https://doi.org/10.5066/P955QRPQ.

Domanski, M.M., Holmes, R.R., and Heal, E.N., 2022b, Dynamic stage to discharge rating model archive: U.S. Geological Survey data release, https://doi.org/10.5066/P9YUV9DG.

U.S. Geological Survey, 2020, USGS water data for the Nation: U.S. Geological Survey National Water Information System database, https://doi.org/10.5066/F7P55KJN.

ISSN 2331-1258 (online)

Contents

Figures

Tables

Conversion Factors

U.S. customary units to International System of Units

Multiply	By	To obtain
	Length	
foot (ft)	0.3048	meter (m)
mile (mi)	1.609	kilometer (km)
	Area	
square mile (mi^2)	259.0	hectare (ha)
square mile (mi^2)	2.590	square kilometer (km^2)
	Flow rate	
cubic foot per second (ft^3/s)	0.02832	cubic meter per second (m^3/s)

Datum

Vertical coordinate information is referenced to the North American Vertical Datum of 1988 (NAVD 88), National Geodetic Vertical Datum of 1929 (NGVD 1929), and World Geodetic System (WGS 1984).

Supplemental Information

A water year is defined as the 12-month period, October 1 through September 30, and is designated by calendar year in which it ends.

Abbreviations

ADCP	acoustic doppler current profiler
DEM	digital elevation model
HEC–RAS	Hydrologic Engineering Center River Analysis System
MSLE	mean squared logarithmic error
USGS	U.S. Geological Survey
UTC	Universal Time Coordinated

Dynamic Rating Method for Computing Discharge from Time-Series Stage Data

By Marian Domanski, Robert R. Holmes, Jr., and Elizabeth N. Heal

Abstract

Ratings are used for a variety of reasons in water-resources investigations. The simplest rating relates discharge to the stage of the river. From a pure hydrodynamics perspective, all rivers and streams have some form of hysteresis in the relation between stage and discharge because of unsteady flow as a flood wave passes. Simple ratings are unable to represent hysteresis in a stage/discharge relation. A dynamic rating method is capable of capturing hysteresis owing to the variable energy slope caused by unsteady momentum and pressure.

A dynamic rating method developed to compute discharge from stage for compact channel geometry, referred to as DYNMOD, previously has been developed through a simplification of the one-dimensional Saint-Venant equations. A dynamic rating method, which accommodates compound and compact channel geometry, referred to as DYNPOUND, has been developed through a similar simplification as a part of this study. The DYNMOD and DYNPOUND methods were implemented in the Python programming language. Discharge time series computed with the dynamic rating method implementations were then compared to simulated discharge time series and discrete discharge measurements made at U.S. Geological Survey streamgage sites.

Four sets of stage and discharge time series were created using one-dimensional unsteady simulation software with compound channel geometry to compare the results of both dynamic rating methods to results from the full one-dimensional shallow water equations. Discharge time series were computed from stage time series using DYNMOD and DYNPOUND. DYNPOUND outperformed DYNMOD in all four scenarios. The minimum and maximum mean squared logarithmic error (MSLE) for the DYNMOD results were 2.75×10^{-2} and 3.40×10^{-2}, respectively. The minimum and maximum MSLE for the DYNPOUND results were 2.51×10^{-7} and 1.91×10^{-4}, respectively.

The dynamic rating methods were calibrated for six U.S. Geological Survey streamgage sites using observed discharge data collected at the sites. The calibration objective for each site was to minimize the MSLE of the discharge computed with the rating method with respect to observed discharge. For each site, the calibration included all field measurements within a selected water year. The DYNMOD method failed to compute discharge for the full calibration time series for three sites. A method fails to compute when the implementation returns a nonfinite value at a time step. Because the values computed for following time steps are dependent on the previous time step, a nonfinite value results in nonfinite values that follow. For the three sites for which DYNMOD computed the complete discharge time series, the minimum MSLE for calibration was 2.19×10^{-3} and the maximum was 9.77×10^{-3}. The MSLE of the DYNPOUND computed discharge calibration time series for the six sites ranged from 3.70×10^{-3} to 1.25. For each site, an event-based time period was selected to compare the discharge time series computed with the dynamic rating methods to discrete discharge field measurements made at the streamgage sites. The DYNMOD-computed discharge time series for the three sites had an MSLE range of 2.76×10^{-3} to 3.14×10^{-2}. The range of MSLE for the six DYNPOUND sites was 3.64×10^{-3} to 7.23×10^{-2}. Although the DYNMOD method outperforms the DYNPOUND method when calibrated streamgage sites are under consideration, the DYNMOD method failed to compute a discharge time series at three of the six sites. The DYNPOUND method, therefore, was more robust than the DYNMOD method. Improvements to the implementation of the DYNPOUND method may improve the accuracy of the method.

Introduction

A relation to estimate discharge using a continuous surrogate measure is termed a "rating." Ratings are used for a variety of reasons in water-resources investigations, but a predominant use of ratings is at streamgages, where autonomously collected stage is converted to discharge by use of a rating. No widely accepted method for direct discrete continuous measurement of discharge is available. In the absence of direct discrete continuous discharge measurements, discharge typically is determined through continuous surrogate measures of one or more variables such as stage, water-surface slope, rate of change in stage, or index velocity, which are collected

at a streamgage. The derivation of discharge through these surrogate variables utilizes various models that will be termed a "rating." The rating is developed and calibrated using discharge measurements collected onsite by field staff.

The simplest rating relates discharge to stage of the river (simple rating). Hydrologists and engineers have long recognized hysteresis (loops) exist in relations between stage and discharge (Jones, 1915; Corbett, 1943; Fread, 1973; Faye and Cherry, 1980; Rantz and others, 1982). From a pure hydrodynamics perspective (ignoring channel-bed mobility), all rivers and streams have some form of hysteresis (loop effect) in the relation between stage and discharge, even in prismatic channels without flood plains, because of unsteady flow as a flood wave passes (fig. 1). The hysteresis is sometimes small enough that it is hidden within the error of the measurements. Likewise, when the time of reporting of the discharge is large enough, the hysteresis averages out. For example, a mean daily discharge will often hide effects of hysteresis that will be more evident in hourly or 15-minute discharge values as explained in Faye and Cherry (1980, p. 19):

> "The hysteretic relation of stage to discharge indicates that estimates of instantaneous dynamic discharge based on rating curves can be significantly in error. On the other hand, estimates of mean dynamic discharge based on rating curves may not be so severely affected by hysteresis because integration of the underestimated flow during the rising stages is frequently compensated for by a corresponding overestimate during falling stages."

For both of these reasons, simple ratings are often adequate for discharge computation.

Simple ratings do not work as well for streamgages on low-gradient streams, streams with variable backwater, streams with large amounts of channel or overbank storage, streams with highly unsteady flow (rapid rises via flood wave movement), or streams with highly mobile beds (Holmes, 2017). In these cases, a complex rating is often required. A complex rating relates discharge to stage and other variables because of the lack of a unique, univariate relation between stage and discharge. Complex rating methods range from simply adding a second independent variable in the process of computing discharge to computer models that solve conservation-of-momentum and conservation-of-mass partial differential equations, which are known as the Saint-Venant equations (French, 1985). Using some simplifying assumptions, Fread (1973) developed what was termed a "dynamic loop" rating method to compute discharge from a time series of stage at a single streamgage for channels with compact geometry (no flood plain). Dynamic loop refers to a rating method that accounts for the variable energy slope defined by Fread (1975, p. 214) as being "associated with the dynamic inertia and pressure forces of the unsteady flood discharge" as opposed to rating loops imposed by alluvial bedform dynamics or scour and fill processes.

This report documents the testing of the Fread (1973) original dynamic loop method and the development and testing of an expansion of that method to include channels with noncompact channel geometry (channels with flood plains). Testing the dynamic rating methods consists of comparing discharge computed using the original and expanded dynamic rating methods to simulated and observed discharge. Simulated discharge was generated using modeling software, Hydrologic Engineering Center River Analysis System (HEC–RAS; U.S. Army Corps of Engineers, 2016), that computes results using the one-dimensional Saint-Venant equations. Field measurements provide the observed discharge measurements at streamgage sites.

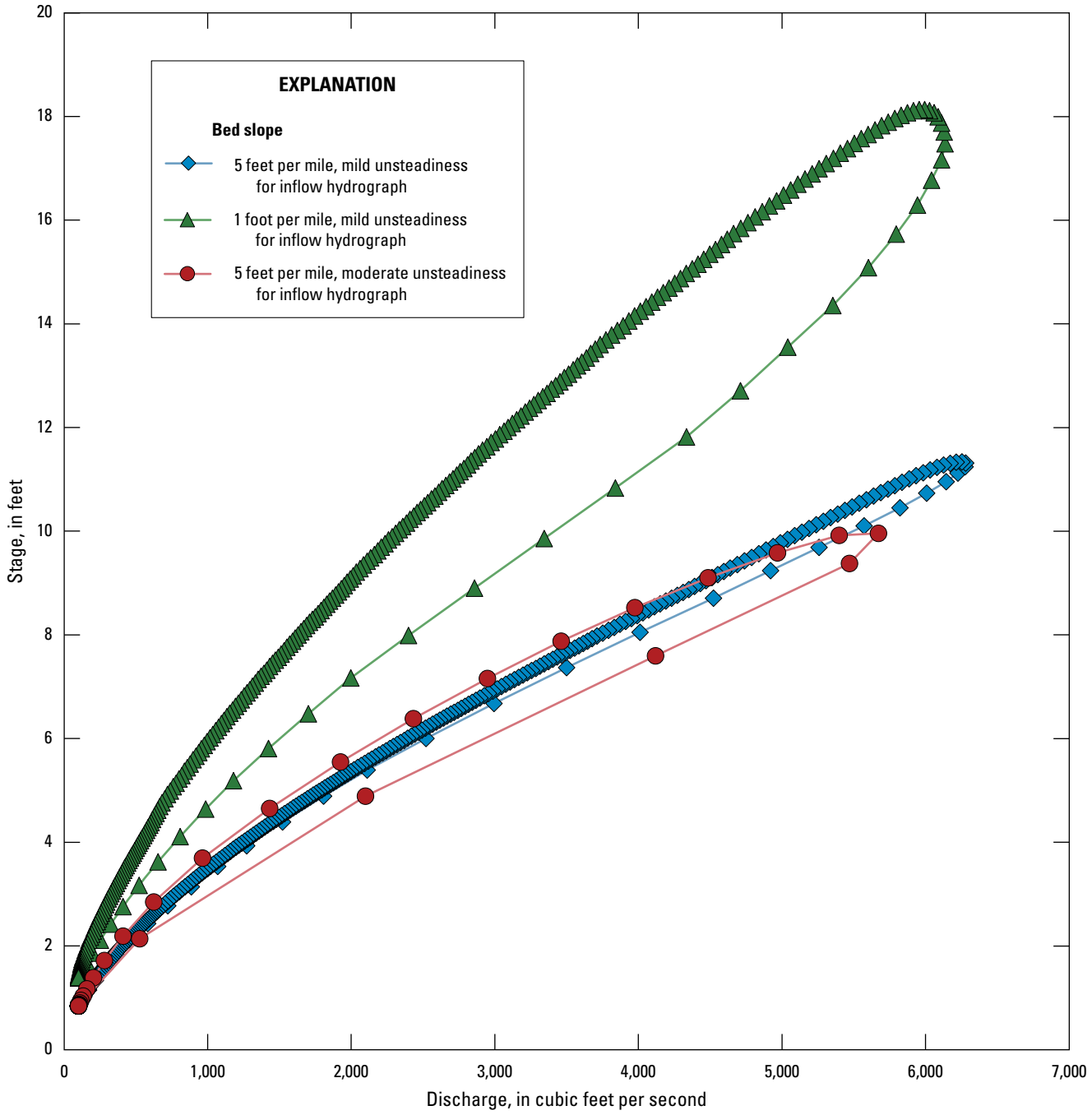

Figure 1. Theoretical determination of the relation between stage and discharge for a 100-foot wide rectangular prismatic channel using a one-dimensional unsteady fully dynamic open-channel hydraulic model with varying bed slopes and rates of unsteadiness (rate of change in local velocity with respect to time) for the inflow hydrograph at the upstream end.

Dynamic Rating Method Theory

The one-dimensional flow in a stream can be described by the Saint-Venant equations (French, 1985), which consist of an equation that represents the one-dimensional streamwise form of the conservation of mass as

$$A\frac{\partial V}{\partial x} + V\frac{\partial A}{\partial x} + B\frac{\partial h}{\partial t} = 0 \quad (1)$$

and an equation that represents the one-dimensional streamwise form of the conservation of momentum as

$$\frac{\partial V}{\partial t} + V\frac{\partial V}{\partial x} + g\left(\frac{\partial y}{\partial x} + S_f - S_0\right) = 0 \quad (2)$$

where

A is the wetted cross-section area of the channel, in square feet;
V is the mean velocity of flow, in feet per second;
x is the streamwise distance along the channel, in feet;
B is the channel width, in feet;
h is the water-surface elevation above a datum plane, in feet;
t is the time, in seconds;
g is the acceleration of gravity, in feet per second squared;
y is the flow depth, in feet;
S_f is the friction slope, in feet per feet; and
S_0 is the bed slope, in feet per feet.

Flow resistance in a channel is often represented by the well-known Manning's equation (Henderson, 1966):

$$Q = \frac{1.49}{n} A R^{2/3} S_f^{1/2} \quad (3)$$

where

Q is the discharge, in cubic feet per second;
n is the Manning's roughness coefficient; and
R is the hydraulic radius, in feet.

If the channel geometry, water-surface elevation, and Manning's roughness coefficient (n) are known, equation 3 only lacks the friction slope (S_f) to compute the discharge. By making simplifying assumptions, Fread (1973) utilized equations 1 and 2 to develop a method to estimate S_f from the time series of stage at a single streamgage and knowledge of how the flood wave moved through a short section of channel at the streamgage location. The assumptions Fread (1973) made are as follows:

1. lateral inflow and outflow are negligible;
2. the channel width is essentially constant ($\partial B/\partial x \approx 0$);
3. energy losses from channel friction and turbulence are described by the Manning's equation;
4. the geometry of the section is essentially permanent (scour and fill are negligible);
5. the bulk of the flood wave is moving approximately as a kinematic wave, which implies S_f is approximately equal to S_0 and the wave propagates only in the downstream direction; and
6. the flow at the section is controlled by the channel geometry, S_f, S_0, and the shape of the flood wave.

Because the method utilizes data at a single streamgage, the above assumptions are used to adjust equations 1 and 2 so that differential terms with respect to the downstream distance, x in ($\partial V/\partial x$, $\partial A/\partial x$, $\partial y/\partial x$), are replaced with approximations that eliminate the need for these terms. We start the process by first rearranging equation 2 as follows:

$$S_f = S_0 - \frac{\partial y}{\partial x} - \frac{V}{g}\frac{\partial V}{\partial x} - \frac{1}{g}\frac{\partial V}{\partial t} \quad (4)$$

The various components that make up S_f are respectively S_0; a pressure term, $\partial y/\partial x$; the convective acceleration of the flow, $V/g\,\partial V/\partial x$; and the local acceleration of the flow, $1/g\,\partial V/\partial t$. Based on assumption 2, $\partial B/\partial x \approx 0$, equation 1 becomes

$$\frac{\partial V}{\partial x} = -\frac{VB}{A}\frac{\partial y}{\partial x} - \frac{B}{A}\frac{\partial h}{\partial t} \quad (5)$$

Placing equation 5 into equation 4 yields the following equation:

$$S_f = S_0 - \frac{\partial y}{\partial x} - \frac{V}{g}\left(-\frac{VB}{A}\frac{\partial y}{\partial x} - \frac{B}{A}\frac{\partial h}{\partial t}\right) - \frac{1}{g}\frac{\partial V}{\partial t} \quad (6)$$

This equation then becomes

$$S_f = S_0 - \frac{\partial y}{\partial x} + \frac{BV^2}{gA}\frac{\partial y}{\partial x} + \frac{BV}{gA}\frac{\partial h}{\partial t} - \frac{1}{g}\frac{\partial V}{\partial t} \quad (7)$$

and through further rearrangement and replacement of V with Q/A becomes

$$S_f = S_0 + \left(\frac{BQ^2}{gA^3} - 1\right)\frac{\partial y}{\partial x} + \frac{BQ}{A^2 g}\frac{\partial h}{\partial t} - \frac{1}{g}\frac{\partial (Q/A)}{\partial t} \quad (8)$$

At this point, the pressure term $\partial y/\partial x$ needs to be replaced with an equivalent expression. Henderson (1966) shows that for a flood wave moving approximately as a kinematic wave (assumption 5), the pressure term can be represented as

$$\frac{\partial y}{\partial x} = -\frac{1}{c}\frac{\partial h}{\partial t} - \frac{2S_0}{3r^2} \quad (9)$$

where

c is the flood wave velocity, in feet per second; and

r is defined as the ratio of S_0 to the average wave slope (S_W).

The flood wave velocity can be represented (Henderson, 1966) as

$$c = \frac{1}{B}\frac{\partial Q}{\partial h} \tag{10}$$

Allowing equation 3 to represent Q results in

$$\frac{\partial Q}{\partial h} = \frac{1.49}{n} S_f^{1/2} \frac{\partial}{\partial h}(A R^{2/3}) \tag{11}$$

Hydraulic radius, R, is defined as the wetted cross-section area divided by the wetted perimeter, P (R=A/P); however, Fread (1973) assumed that hydraulic radius could be approximated by the hydraulic depth, which is the wetted cross-section area (A) divided by the width of the channel at the water surface (top width; B). Using this assumption, equation 11 becomes

$$\frac{\partial Q}{\partial h} = \frac{1.49}{n} S_f^{1/2} \frac{A^{2/3}}{B^{2/3}} \left(\frac{5}{3}\frac{\partial A}{\partial h} - \frac{2}{3}\frac{A}{B}\frac{\partial B}{\partial h} \right) \tag{12}$$

According to Henderson (1966), the change in cross-section area with respect to stage is equal to the top width (eq. 13):

$$\frac{\partial A}{\partial h} = B \tag{13}$$

Combining equations 3, 10, 12, and 13 and simplifying yields the following:

$$c = \left(\frac{5}{3} - \frac{2}{3}\frac{A}{B^2}\frac{\partial B}{\partial h} \right) \frac{Q}{A}. \tag{14}$$

The celerity coefficient (K_c) is

$$K_c = \frac{5}{3} - \frac{2}{3}\frac{A}{B^2}\frac{\partial B}{\partial h} \tag{15}$$

resulting in

$$c = K_c \frac{Q}{A} \tag{16}$$

It should be noted that this work does not follow Fread's (1973) assumption that $R \approx A/B$, but rather stays with the true definition of hydraulic radius, $R = A/P$. For this situation, equation 15 becomes

$$K_c = \frac{5}{3} - \frac{2}{3}\frac{A}{BP}\frac{\partial P}{\partial h} \tag{17}$$

Fread's (1973) assumption works well with large channels, but the methods developed in this report are applicable to a range of channel sizes.

The second term in equation 9 is a small correction to account for the fact that flood waves do not move as a kinematic wave. The second term is dependent on a value of r that requires not only determination of S_0 but also the S_W. Information from a typical flood wave at the streamgage is needed to estimate the S_W as the height of a flood wave divided by the half length of the flood wave, which is represented by the following equation:

$$S_W = \frac{h_p - h_0}{\tau V_k} \tag{18}$$

where

h_p is the stage at the peak of a typical flood, in feet;

h_0 is the stage prior to beginning of the typical flood, in feet;

V_k is the velocity of the flood wave, in feet per second; and

τ is the elapsed time between the beginning of the typical flood to the peak of the flood, in seconds.

The velocity of the flood wave is estimated from equation 16 with the assumption that K_c=1.3 (Fread, 1973) and average values used for the flow and area such that

$$V_K = 1.3\frac{Q_P + Q_0}{2\overline{A}} \tag{19}$$

where

Q_p is the peak discharge for a typical flood, in cubic feet per second;

Q_0 is the discharge prior to the beginning of the typical flood, in cubic feet per second; and

$\overline{A}$ is the wetted cross-section area associated with the average stage, $(h_p + h_0)/2$.

Utilizing equations 18 and 19, the following relation is determined as

$$r = 0.65\frac{(Q_p + Q_0)}{(h_p - h_0)\overline{A}}\tau S_0 \tag{20}$$

Given the developments shown through equations 9–20, equation 6 can now be revised through appropriate substitutions and finite difference approximations to obtain

$$S_f = S_0 + \left[\frac{A_j}{K_j Q_j} + \left(1 - \frac{1}{K_j}\right)\frac{B}{gA_j^2}\right]\frac{\left(h_j - h_{j-1}\right)}{\Delta t} - \frac{Q_j/A_j - Q_{j-1}/A_{j-1}}{g\Delta t} + \frac{2S_0}{3r^2}\left(1 - \frac{BQ_j^2}{gA_j^3}\right) \quad (21)$$

where

j is for the current time, and
"$j-1$" is for time $t-\Delta t$.

Equation 21 is an equation for S_f, which is changing with changes in discharge. Using equation 21 with equation 3 allows for the discharge to be dynamically determined from a time series of stage. Because discharge at the current time (Q_j) is on both sides of the equal sign, an implicit solution must be employed to solve for Q_j.

The conservation of momentum and mass equations (eqs. 1 and 2) use mean channel velocity to develop equation 21, which is a reasonable representation of the flow physics for compact geometry channels (channel with no flood plains). For channels with flood plains, equations 1 and 2 need adjustment to account for changes in velocity across the channel.

The method developed for compound channel geometry is derived as follows. The equations for one-dimensional conservation of mass and momentum take the form of equations 22 and 23, respectively (Cunge and others, 1980).

$$\frac{\partial A}{\partial t} + \frac{\partial Q}{\partial x} = 0 \quad (22)$$

$$\frac{\partial Q}{\partial t} + \frac{\partial\left(\beta Q^2 / A\right)}{\partial x} + gA\frac{\partial h}{\partial x} + gAS_f = 0 \quad (23)$$

The variable β is the non-uniform velocity distribution coefficient and is defined by equation 24 for a cross section divided into N discrete subsections, where the subscript i is the ith discrete subsection. Equation 24 is derived under the assumptions that

- the discharge for the total cross section is equal to the sum of discharges in each subsection, and
- S_f for the total cross section is equal to S_f for each subsection.

$$\beta = \frac{A}{K^2}\sum_i^N \frac{K_i^2}{A_i} \quad (24)$$

In equation 24, K is conveyance and is calculated by equation 25 for the whole cross section and equation 26 for the ith subsection.

$$K = \frac{1.486}{n} AR^{2/3} \quad (25)$$

$$K_i = \frac{1.486}{n_i} A_i R_i^{2/3} \quad (26)$$

The water-surface elevation slope, $\frac{\partial h}{\partial x}$, which appears in the third term in equation 23, is equivalent to the slope of the water depth minus S_0, as shown in equation 27.

$$\frac{\partial h}{\partial x} = \frac{\partial y}{\partial x} - S_o \quad (27)$$

Taking the partial derivative with respect to x in the second term in equation 23 yields

$$\frac{\partial\left(\beta Q^2 / A\right)}{\partial x} = \frac{Q^2}{A}\frac{\partial \beta}{\partial x} + \beta\frac{2Q}{A}\frac{\partial Q}{\partial x} - \beta\frac{Q^2}{A^2}\frac{\partial A}{\partial x} \quad (28)$$

Using the chain rule, the partial derivative of β with respect to x yields $\frac{\partial \beta}{\partial x} = \frac{\partial \beta}{\partial y}\frac{\partial y}{\partial x}$. If $\frac{\partial \beta}{\partial y}$, the change in nonuniform velocity distribution coefficient with respect to depth, and $\frac{\partial y}{\partial x}$, the change in depth with respect to longitudinal distance, are both assumed to be much less than 1, then the product of the two is considered to be negligible with respect to the rest of the terms, so the term $\frac{Q^2}{A}\frac{\partial \beta}{\partial x}$ is dropped. The above equation reduces to

$$\frac{\partial\left(\beta Q^2 / A\right)}{\partial x} \approx \beta \frac{2Q}{A}\frac{\partial Q}{\partial x} - \beta \frac{Q^2}{A^2}\frac{\partial A}{\partial x}. \quad (29)$$

Moving the partial derivative of cross-sectional area with respect to time to the right-hand side of equation 22 yields

$$\frac{\partial Q}{\partial x} = -\frac{\partial A}{\partial t}. \quad (30)$$

Using the chain rule in taking the partial derivative of A with respect to x, and using the assumption of $\frac{\partial A}{\partial y} = B$ (eq. 13), yields

$$\frac{\partial A}{\partial x} = \frac{\partial A}{\partial y}\frac{\partial y}{\partial x} = B\frac{\partial y}{\partial x}. \quad (31)$$

Substituting equations 30 and 31 into equation 29 yields

$$\frac{\partial\left(\beta Q^2 / A\right)}{\partial x} = -\beta \frac{2Q}{A}\frac{\partial A}{\partial t} - \beta B \frac{Q^2}{A^2}\frac{\partial y}{\partial x}. \quad (32)$$

Discharge is related to conveyance and S_f by $Q = KS_f^{1/2}$. Solving this equation for S_f gives S_f in terms of discharge and conveyance.

$$S_f = \left(\frac{Q}{K}\right)^2 \quad (33)$$

Substituting equations 27, 32, and 33 into equation 23, dividing through by gA, and rearranging the result yields

$$\frac{1}{gA}\frac{\partial Q}{\partial t} - \beta \frac{2Q}{gA^2}\frac{\partial A}{\partial t} + \left(1 - \beta B \frac{Q^2}{gA^3}\right)\frac{\partial y}{\partial x} + \left(\frac{Q}{K}\right)^2 - S_o = 0. \quad (34)$$

As in the compact geometry method described previously, the compound geometry method uses equation 9 to compute the pressure term $\frac{\partial y}{\partial x}$. Unlike the compact geometry method, the compound channel method uses the following relation to compute wave celerity:

$$c = \frac{dQ}{dA} \quad (35)$$

Under the kinematic wave assumption, S_f is equal to S_0, so discharge is related to conveyance by $Q = KS_0^{1/2}$ (Henderson, 1966). Taking the derivative of Q in this relation gives

$$c = S_0^{1/2}\frac{dK}{dA}. \quad (36)$$

Because all variables in equation 34 are either Q, known functions of h, or known constants, equation 34 is a nonlinear function of Q. The development of a discretized version of equation 34 and a solution method are discussed in the next section.

Solution Method

Both methods described in this report were implemented in the Python programming language. DYNMOD is the dynamic rating method that computes discharge from stage for compact channel geometry, whereas DYNPOUND is the newly developed method that solves for discharge in compact and compound channels. The computation procedure for DYNMOD uses the Newton-Raphson numerical method (Fread, 1973). The following is a discussion of the DYNPOUND numerical solution technique.

To compute an unknown discharge for a time t_j, which occurs sometime after a time t_{j-1}, the method requires the following:

- known constants, which are S_0, r, and g;
- a known discharge value Q_{j-1} observed at a time t_{j-1};
- a known stage value h_{j-1} observed at a time t_{j-1};
- a known stage value h_j observed at a time t_j; and
- A, B, β, and K as a known function of stage.

The method to compute discharge at a site with compound channel geometry contains continuous derivatives that need to be discretized to determine discharge time-series values. Beginning with the derivative in the first term of equation 34, $\frac{\partial Q}{\partial t}$ can be discretized as

$$\frac{\partial Q}{\partial t} \approx \frac{Q_j - Q_{j-1}}{t_j - t_{j-1}}. \quad (37)$$

The second term of equation 34, $\frac{\partial A}{\partial t}$, becomes

$$\frac{\partial A}{\partial t} \approx \frac{A_j - A_{j-1}}{t_j - t_{j-1}}, \quad (38)$$

where

A_j is the cross-sectional area for stage h_j.

The pressure term $\frac{\partial y}{\partial x}$ in equation 34 is computed from equation 9, which requires the computation of c and the derivative $\frac{\partial h}{\partial t}$. Equation 36 is used to compute c and contains the derivative $\frac{dK}{dA}$, which becomes

$$\frac{dK}{dA} \approx \frac{\Delta K_j}{\Delta A_j}, \tag{39}$$

where

$$\Delta K_j = K_{h_j + \frac{1}{2}\Delta h} - K_{h_j - \frac{1}{2}\Delta h} \text{ and} \tag{40}$$

$$\Delta A_j = A_{h_j + \frac{1}{2}\Delta h} - A_{h_j - \frac{1}{2}\Delta h}. \tag{41}$$

In the current implementation of the method, Δh = 0.01 foot. Once the derivative of K with respect to stage is computed, equation 36 is used to compute the c. The partial derivative of stage with respect to time is computed as

$$\frac{\partial h}{\partial t} \approx \frac{h_j - h_{j-1}}{t_j - t_{j-1}}. \tag{42}$$

The discrete form of equation 9 becomes

$$\frac{\partial y}{\partial x} \approx -\frac{1}{S_0^{1/2}} \frac{\Delta h}{\Delta K_j} \frac{h_j - h_{j-1}}{t_j - t_{j-1}} - \frac{2S_0}{3r^2}. \tag{43}$$

Substituting all discrete approximations of derivatives into equation 34 yields equation 44.

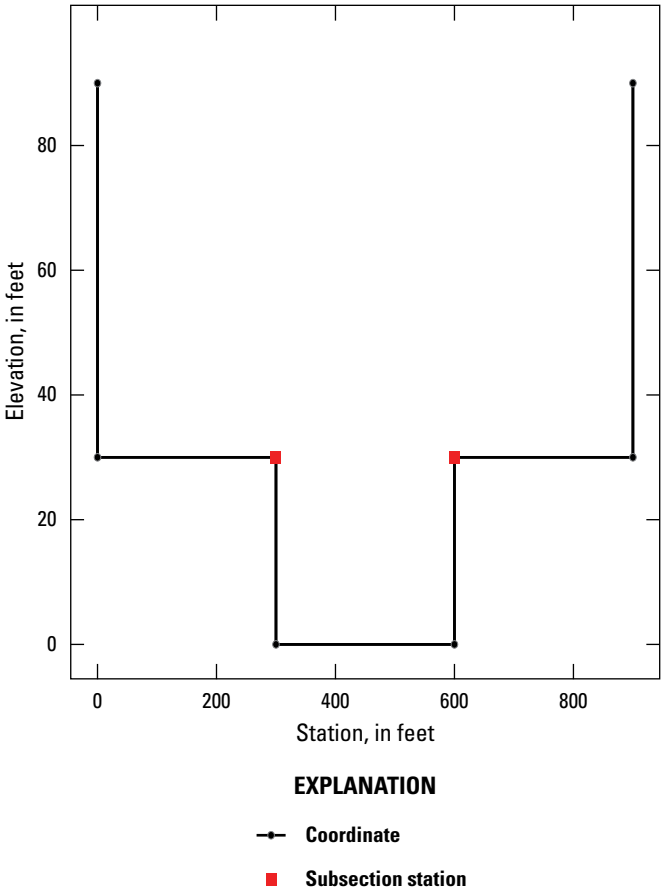

Figure 2. Representative cross section for simulated test datasets.

$$\frac{1}{gA_j} \frac{Q_j - Q_{j-1}}{t_j - t_{j-1}} - \beta_j \frac{2Q_j}{gA_j^2} \frac{A_j - A_{j-1}}{t_j - t_{j-1}} - \left(1 - \beta_j B_j \frac{Q_j^2}{gA_j^3}\right)\left(\frac{1}{S_0^{1/2}} \frac{\Delta A}{\Delta K_j} \frac{h_j - h_{j-1}}{t_j - t_{j-1}} + \frac{2S_0}{3r^2}\right) + \left(\frac{Q_j}{K_j}\right)^2 - S_0 = 0 \tag{44}$$

Equation 44 is a nonlinear function of Q_j because all other values are known. The root of equation 44, and thus the value of Q_j, is determined using the secant method (Dahlquist and Björck, 1974).

These solution methods for the compact (DYNMOD) and compound (DYNPOUND) channel geometries were implemented in the Python programming language. The results shown in this report were computed using the Python implementation.

Evaluation Using Model-Generated Test Scenarios

Simulated scenario test datasets were created from one-dimensional unsteady Hydrologic Engineering Center River Analysis System (HEC–RAS; U.S. Army Corps of Engineers, 2016) simulation results. The purpose of creating the simulated test datasets is to compare the results computed with both dynamic rating methods (DYNMOD and DYNPOUND) described in this report to results computed using the one-dimensional unsteady shallow water equations, of which the dynamic rating methods are a simplification. The simulated test datasets can be found in the U.S. Geological Survey (USGS) data release by Domanski and others (2022a), and the source code and calibration parameters for the DYNMOD and DYNPOUND rating methods, along with the HEC-RAS project files, are available from the USGS data release by Domanski and others (2022b).

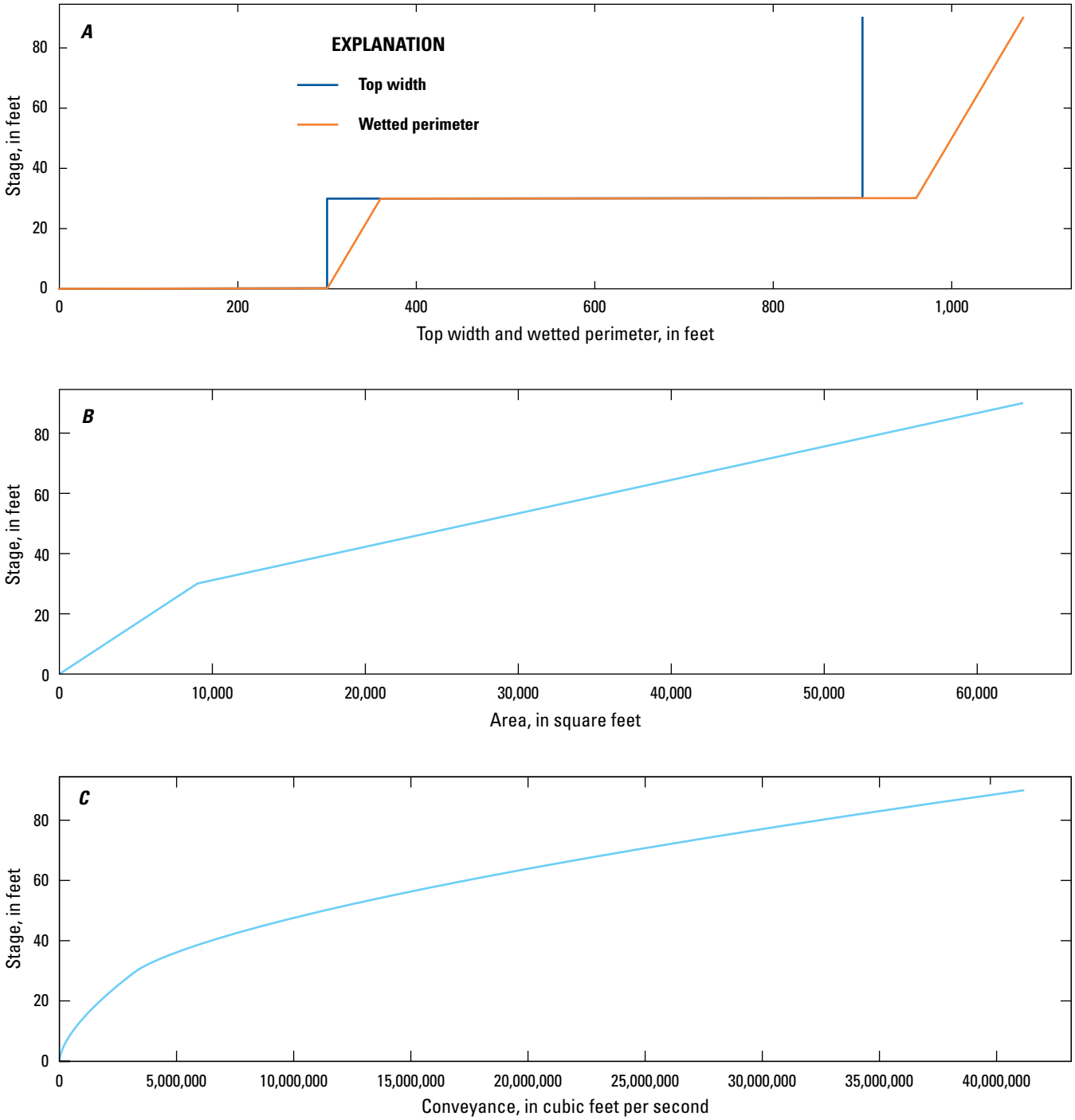

Figure 3. Stage plotted against four variables. *A*, Top width and wetted perimeter. *B*, Area. *C*, Conveyance.

A prismatic channel geometry (fig. 2), with flood plains on each side and a main channel with a total length of 80 miles, was used for four different scenarios with different combinations of S_0 and r (table 1). An n value of 0.035 was used in all cross sections. The cross sections in the channels were split into three subsections to allow for computation of the β and to smooth out the conveyance/stage relation (fig. 3). The subsection stationing includes the two bank stations so that two subsections contain the left and right overbank areas and one subsection contains the main channel.

Different inflow hydrographs were developed for the evaluation to test a range of unsteadiness in the simulated responses from the three computation methods: HEC–RAS,

Table 1. Bed slope and ratio of bed slope to average wave slope of simulated test data scenarios.

[*r*, ratio of bed slope to average wave slope]

Scenario	Bed slope	*r*
1	0.0001	10
2	0.0001	100
3	0.001	10
4	0.001	100

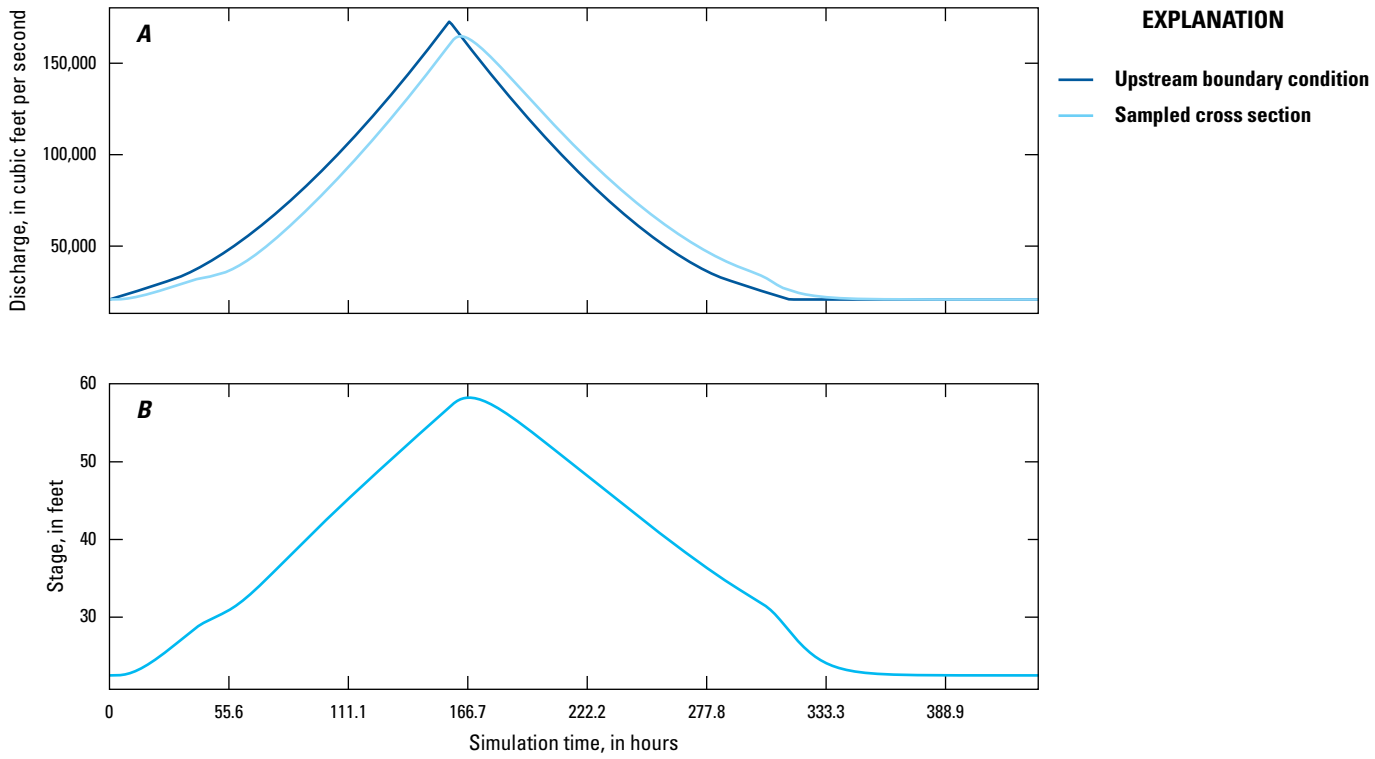

Figure 4. Simulated time series for simulated test scenario 1. *A*, Discharge. *B*, Stage.

DYNMOD, and DYNPOUND. A normal depth boundary condition was used at the downstream end in each scenario with the appropriate S_0 assigned to the normal depth relation.

All scenarios were simulated in HEC–RAS. The HEC–RAS computed stage and discharge time series at the cross-section midway (40 miles from the inflow point) between the most upstream and most downstream cross sections of the 80-mile reach were extracted and used for computation and comparison of the discharge with the dynamic rating methods. The midpoint cross section was selected to reduce the effects of the boundary conditions on the simulation results. The Manning's *n*, S_0, and *r* values used in the development of the HEC–RAS scenarios were assigned to the parameters in the dynamic rating discharge computations.

Dataset Development

The width of the main channel of the simulation cross section was 300 ft, the flood plains have a total width of 600 ft, and the total width of the cross section was 900 ft. The bankfull depth of the main channel was 30 ft. The subsection stations coincide with the bank stations at 300 and 600 ft (fig. 2). A Manning's *n* value of 0.035 was used in the cross section for all scenarios.

Four hydrographs, which were used as upstream boundary conditions for each scenario, were developed to simulate stage and discharge time series under varied channel slope and unsteadiness conditions in the test scenarios (figs. 4–7; Domanski and others, 2022b). The value of unsteadiness can be characterized by the ratio of bed slope to average wave slope (*r*). The larger the value of *r* for a particular bed

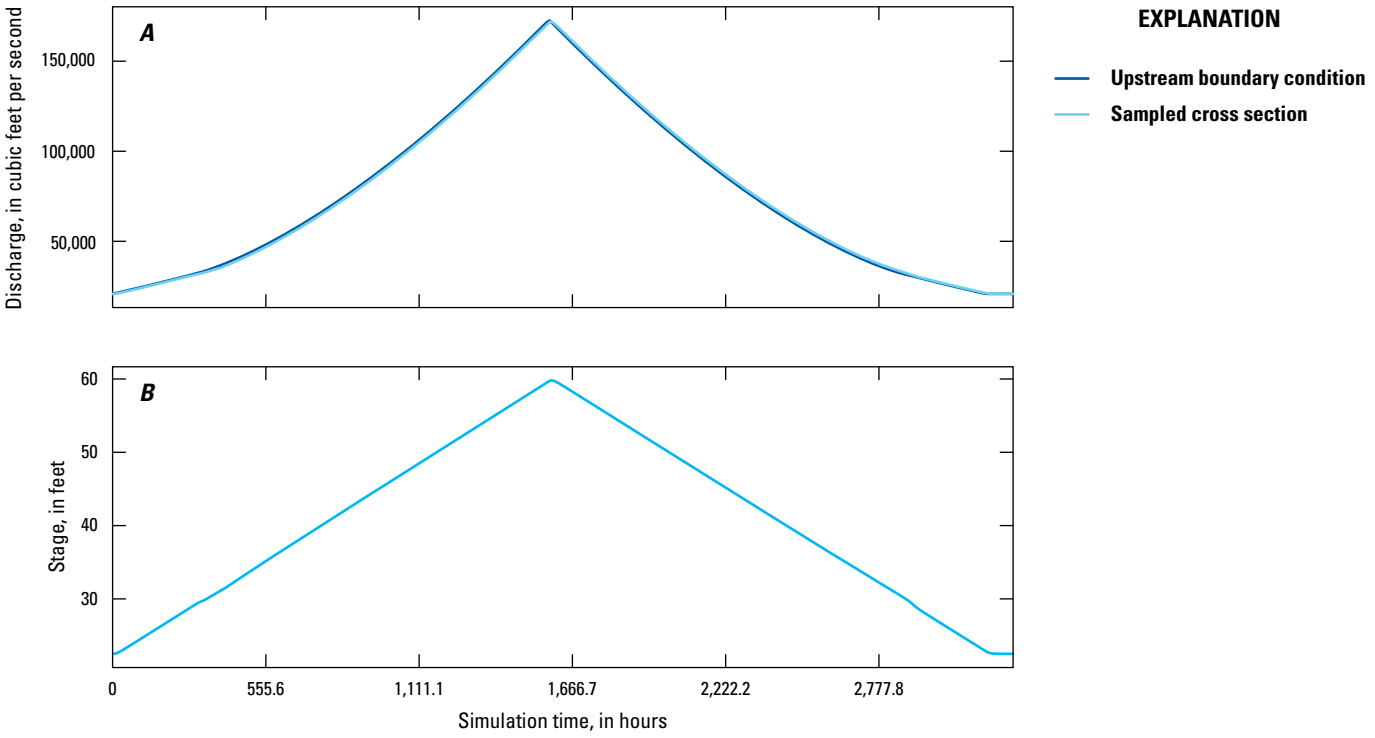

Figure 5. Simulated time series for simulated test scenario 2. *A*, Discharge. *B*, Stage.

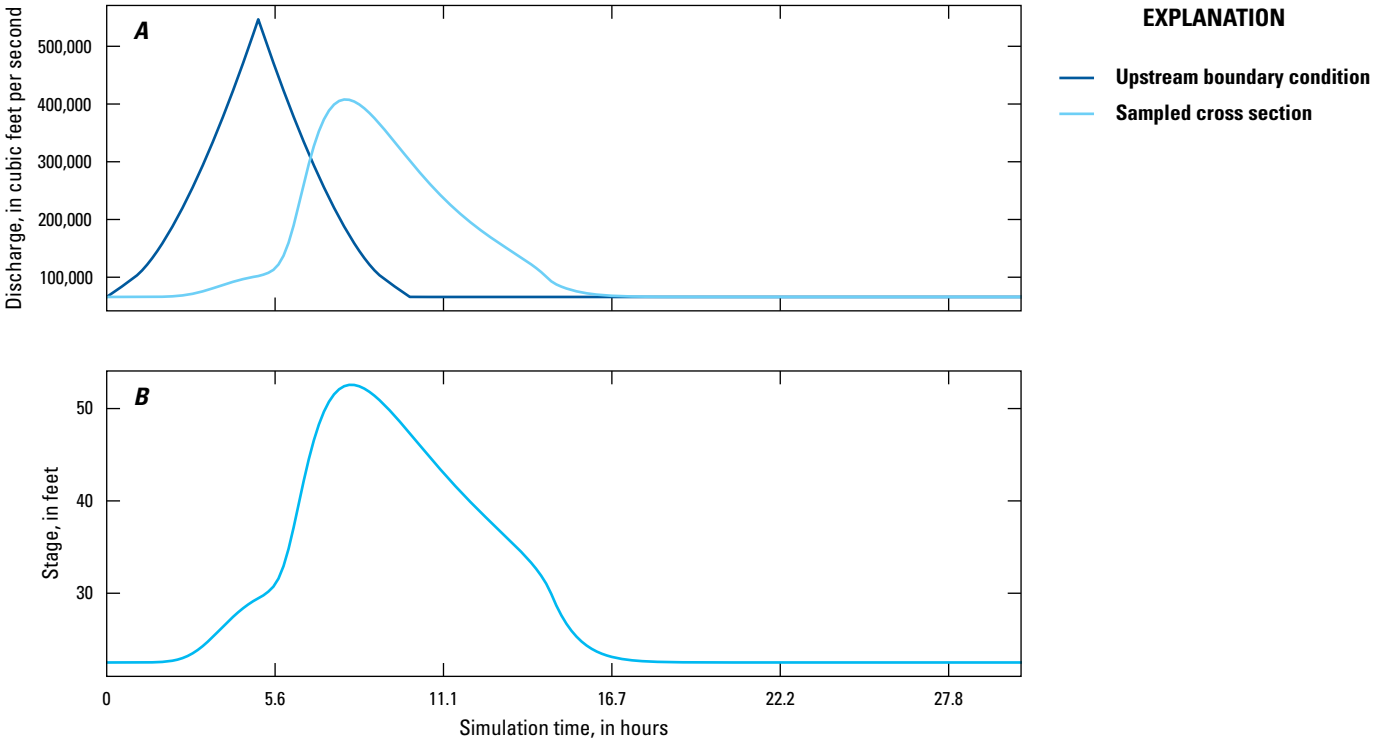

Figure 6. Simulated time series for simulated test scenario 3. *A*, Discharge. *B*, Stage.

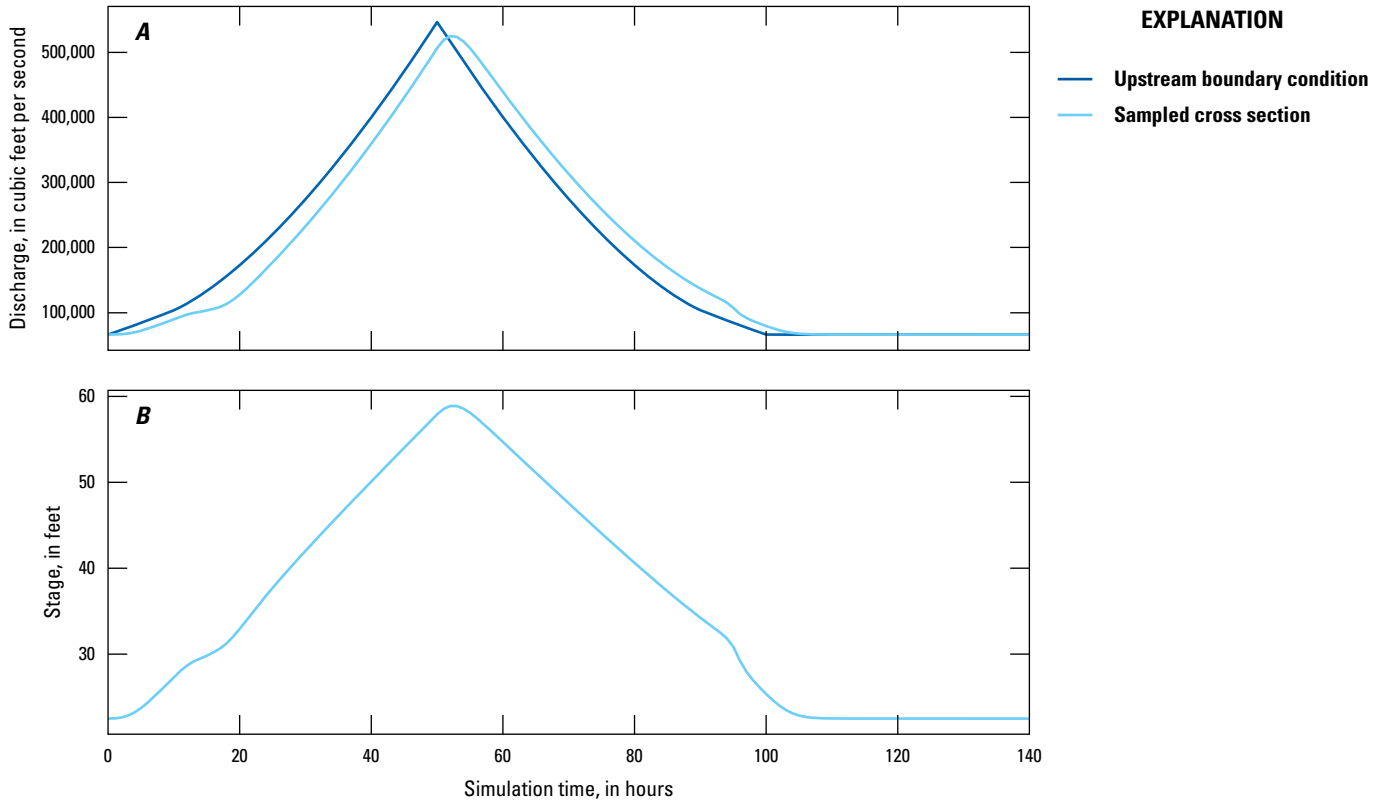

Figure 7. Simulated time series for simulated test scenario 4. *A*, Discharge. *B*, Stage.

Table 2. Performance statistics for the DYNMOD and DYNPOUND discharge computation methods.

[DYNMOD, the dynamic rating method that computes discharge from stage for compact channel geometry; DYNPOUND, the newly developed method that solves for discharge in compact and compound channels; MSLE, mean squared logarithmic error]

Scenario	DYNMOD			DYNPOUND		
	Mean percent error	Maximum absolute percent error	MSLE	Mean percent error	Maximum absolute percent error	MSLE
1	−3.91	49.3	3.40×10^{-2}	0.444	10.4	1.91×10^{-4}
2	−5.81	45.7	3.35×10^{-2}	−0.0100	0.723	8.24×10^{-7}
3	−1.16	41.2	2.75×10^{-2}	0.0370	2.73	4.31×10^{-5}
4	−4.78	43.4	3.13×10^{-2}	−0.00572	0.358	2.51×10^{-7}

slope, the lower the unsteadiness of the hydrograph; that is, the time from the onset of the flooding to the flood peak increases with increasing value of *r*. To determine the actual inflow hydrographs used for the scenarios, a flood wave slope was computed from a bed slope and an assumed value of *r* (table 1). The rising and falling limbs of the stage hydrograph were computed using the slope of the flood wave between the end points of 75 percent of the bankfull main channel depth (22.5 ft) to the peak stage (60.0 ft). The peak stage was chosen such that the total wetted area in the flood plain equaled the wetted area in the channel. From the stage hydrograph, Manning's equation was used to compute the discharge hydrographs for the upstream boundary condition.

Evaluation

Both the DYNMOD and DYNPOUND methods performed well in comparison to the full one-dimensional unsteady flow equations within HEC–RAS because the mean percent error was within about 5.8 percent (table 2). The method developed for compound channel geometry (DYNPOUND) shows an improvement over the existing method for

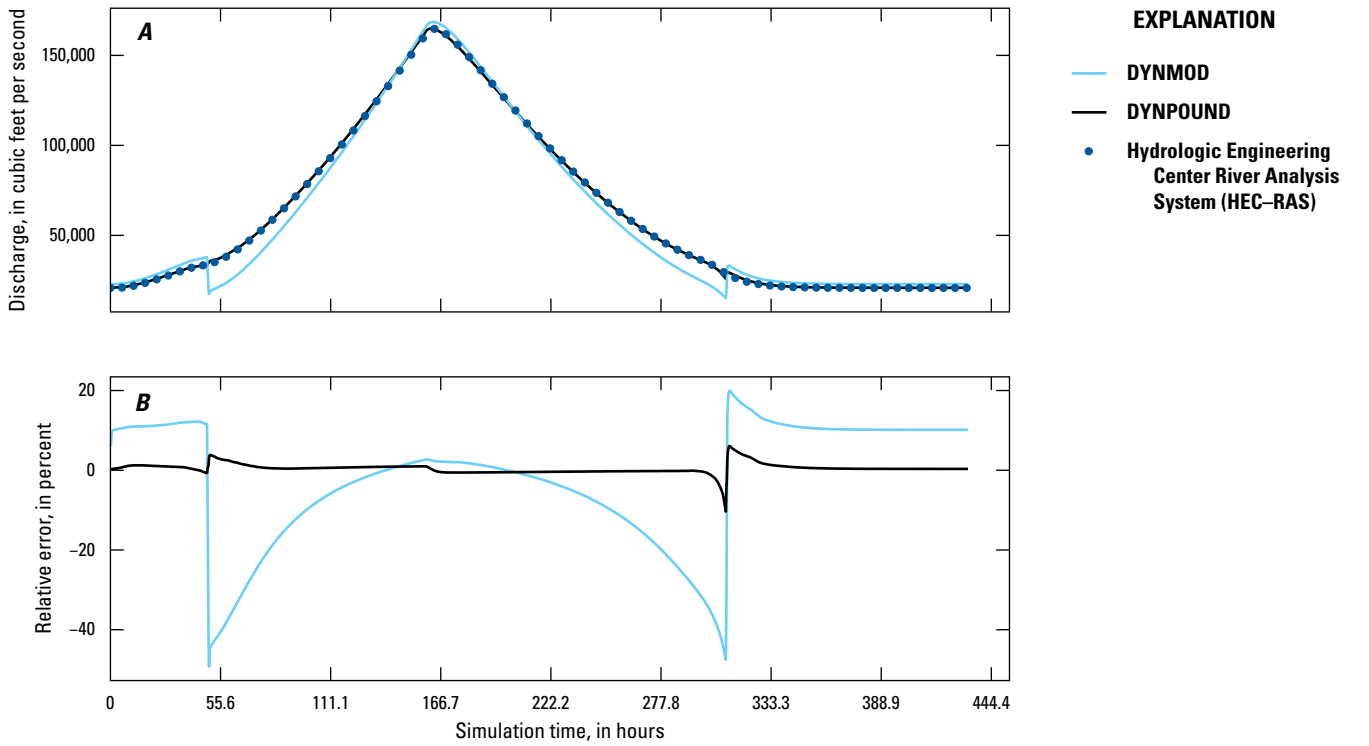

Figure 8. Time series for simulated scenario 1. *A*, Discharge computed with the DYNMOD and DYNPOUND methods; *B*, Percent error of the DYNMOD and DYNPOUND computed discharge; DYNMOD, the dynamic rating method that computes discharge from stage for compact channel geometry; DYNPOUND, the newly developed method that solves for discharge in compact and compound channels.

compact geometry (DYNMOD). The discharge computed with the DYNPOUND method is closer to the HEC–RAS simulated discharge in both maximum absolute and mean percent errors (table 2).

Scenarios 1 (fig. 4) and 3 (fig. 6) have *r* values of 10 (table 1), and therefore high unsteadiness, and show pronounced hysteresis in the stage versus discharge curves. Scenarios 2 (fig. 5) and 4 (fig. 7), which have *r* values of 100 (table 1), do not show hysteresis.

In all test scenarios, jumps in the discharge computed with the DYNMOD method are observed in the time series. The first jump from a higher to a lower discharge takes place when the stage rises from below to above the channel bank elevation, and the second jump from a lower to higher discharge takes place once the elevation falls below the bank elevation. This jump takes place because of abrupt changes in the relations of top width, wetted perimeter, and area with stage, as indicated in figure 3.

Overall, the magnitude of the mean percent error is much greater in the results computed with the DYNMOD method when compared to the mean percent error in the results computed with the DYNPOUND method. The error is smaller in the time series computed with the DYNPOUND method because this method relies on the conveyance, as well as area and top width (see equation 33). The function of conveyance with stage can be developed so that changes are less abrupt by creating subsections in the cross section, as was done for the simulated test scenarios.

In all scenarios, the DYNMOD computed discharge has a maximum percent error ranging from about 40 to almost 50 percent that takes place when the water surface rises above and falls below the channel bank elevations. The DYNMOD method performs about the same in all four test scenarios, whereas the DYNPOUND method performs better in scenarios 2 and 4 than it does in scenarios 1 and 3 (table 2), both of which effectively have one-to-one stage/discharge relations.

Scenario 1

The scenario 1 (fig. 8) stage/discharge relation indicates hysteresis in the HEC–RAS results owing to unsteady flow effects captured in the simulation (fig. 9). For the DYNMOD computed time series, the mean percent error is −3.91 percent, and the mean squared logarithmic error (MSLE) is 3.40×10^{-2} (table 2). The time series computed with DYNPOUND has a mean percent error of 4.44×10^{-1} percent and a MSLE of 1.91×10^{-4} (table 2).

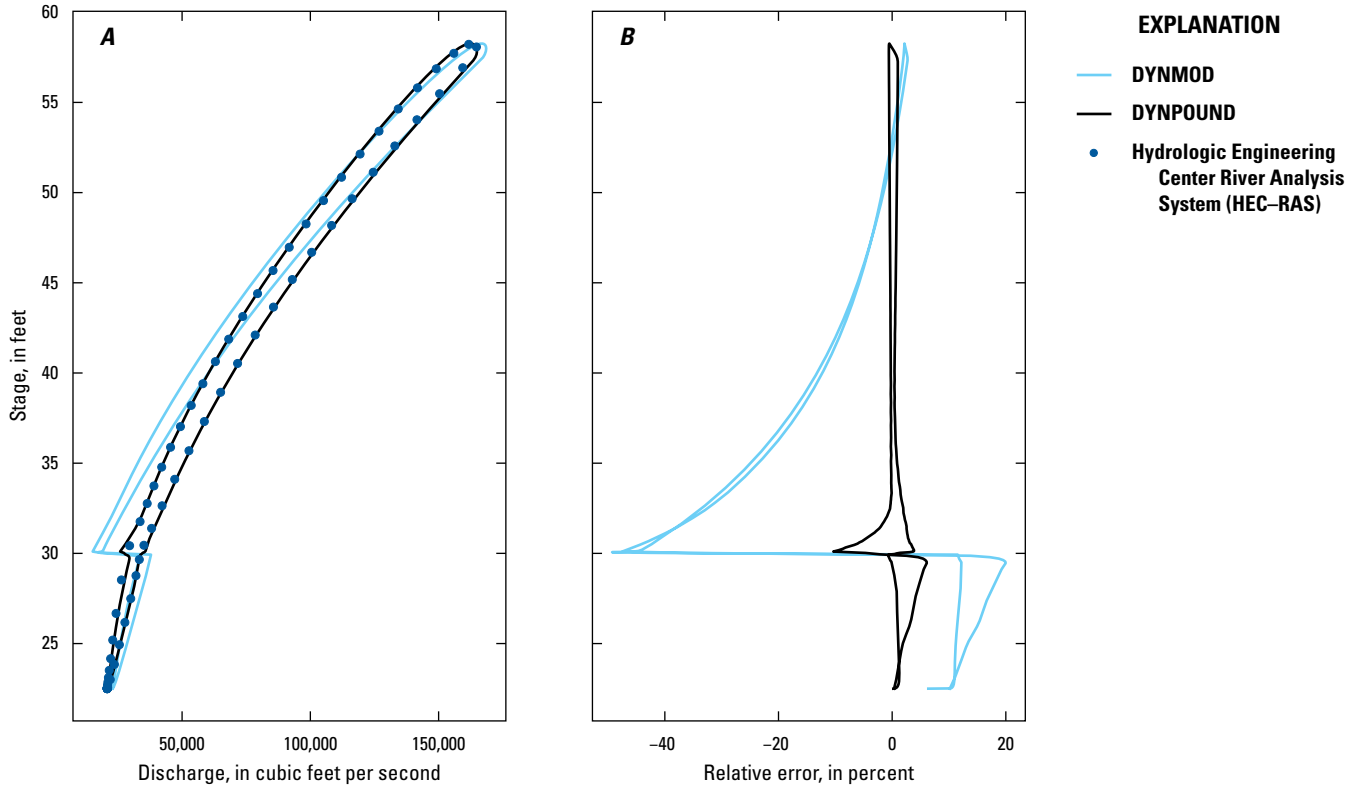

Figure 9. Relation between stage and computed discharge for simulated scenario 1. *A,* DYNMOD and DYNPOUND computed discharge; *B,* Percent error of the DYNMOD and DYNPOUND computed discharge; DYNMOD, the dynamic rating method that computes discharge from stage for compact channel geometry; DYNPOUND, the newly developed method that solves for discharge in compact and compound channels.

Scenario 2

The results of scenario 2 indicate a lack of hysteresis of the computed hydrograph but substantial relative error in the DYNMOD solution compared to the HEC–RAS and DYNPOUND methods (figs. 10 and 11). The stage/discharge relation of the HEC–RAS results for scenario 2 is effectively one-to-one because the distance between the discharge values computed at a given stage is small (fig. 11). For the DYNMOD computed time series, the mean percent error was −5.81 percent, and the MSLE was 3.35×10^{-2} (table 2). The error in the DYNPOUND computed discharge was substantially lower and had a mean percent error of -1.00×10^{-2} percent and a MSLE of 8.24×10^{-7}.

Scenario 3

The stage/discharge relation of the HEC–RAS computed values for scenario 3 shows hysteresis (figs. 12 and 13). The mean percent error for the DYNMOD computed discharge was −1.16 percent, and the MSLE was 2.75×10^{-2} (table 2). The mean percent error for the DYNPOUND computed discharge was 0.0370 percent, and the MSLE was 4.31×10^{-5}.

Scenario 4

The stage/discharge relation of the scenario 4 time series (fig. 14) as computed using HEC–RAS does not show hysteresis and can effectively be considered a one-to-one relation (fig. 15). The mean percent error for the DYNMOD computed discharge was −4.78 percent, and the MSLE is 3.13×10^{-2} (table 2). The mean percent error for the DYNPOUND computed discharge was −0.00572 percent, and the MSLE was 2.51×10^{-7}.

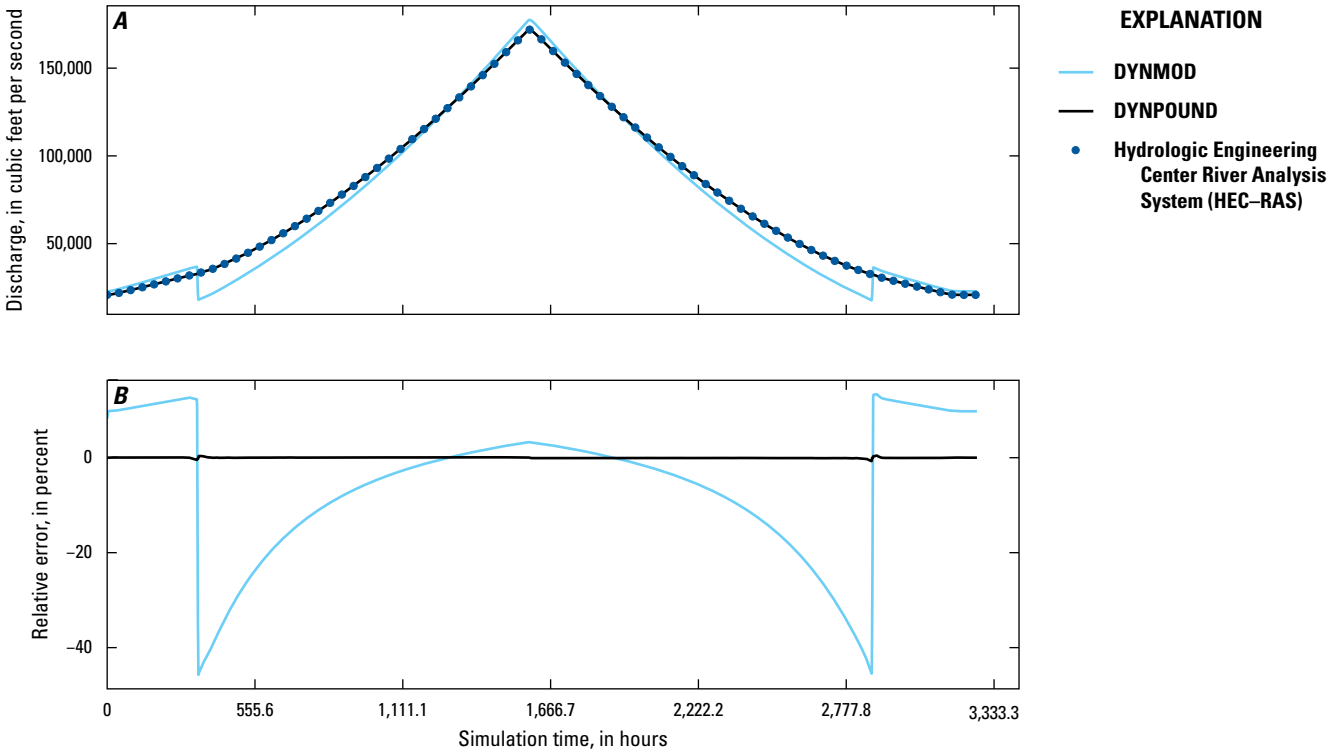

Figure 10. Time series for simulated scenario 2. *A*, Discharge computed with the DYNMOD and DYNPOUND methods; *B*, Percent error of the DYNMOD and DYNPOUND computed discharge time series; DYNMOD, the dynamic rating method that computes discharge from stage for compact channel geometry; DYNPOUND, the newly developed method that solves for discharge in compact and compound channels.

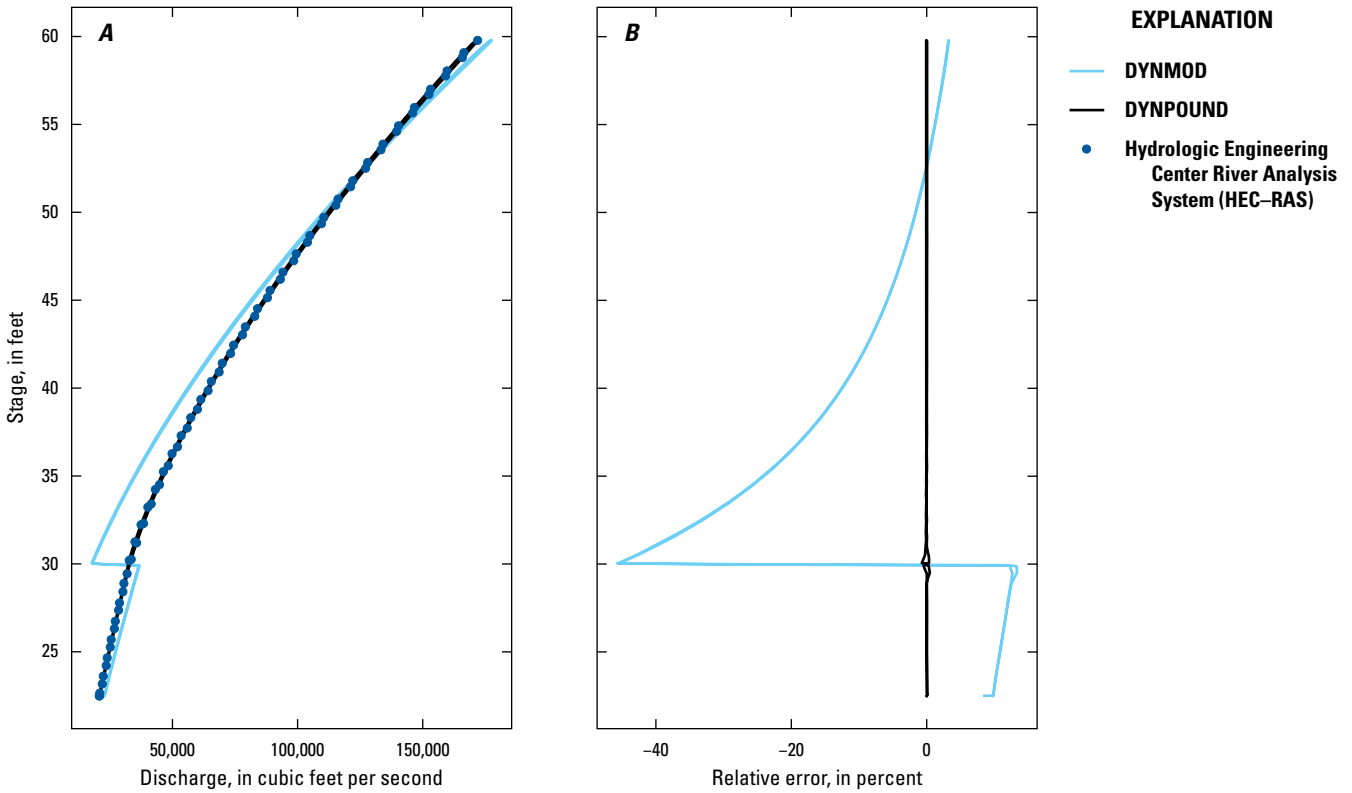

Figure 11. Relation between stage and computed discharge for simulated scenario 2. *A,* DYNMOD and DYNPOUND computed discharge; *B,* Percent error of the DYNMOD and DYNPOUND computed discharge; DYNMOD, the dynamic rating method that computes discharge from stage for compact channel geometry; DYNPOUND, the newly developed method that solves for discharge in compact and compound channels.

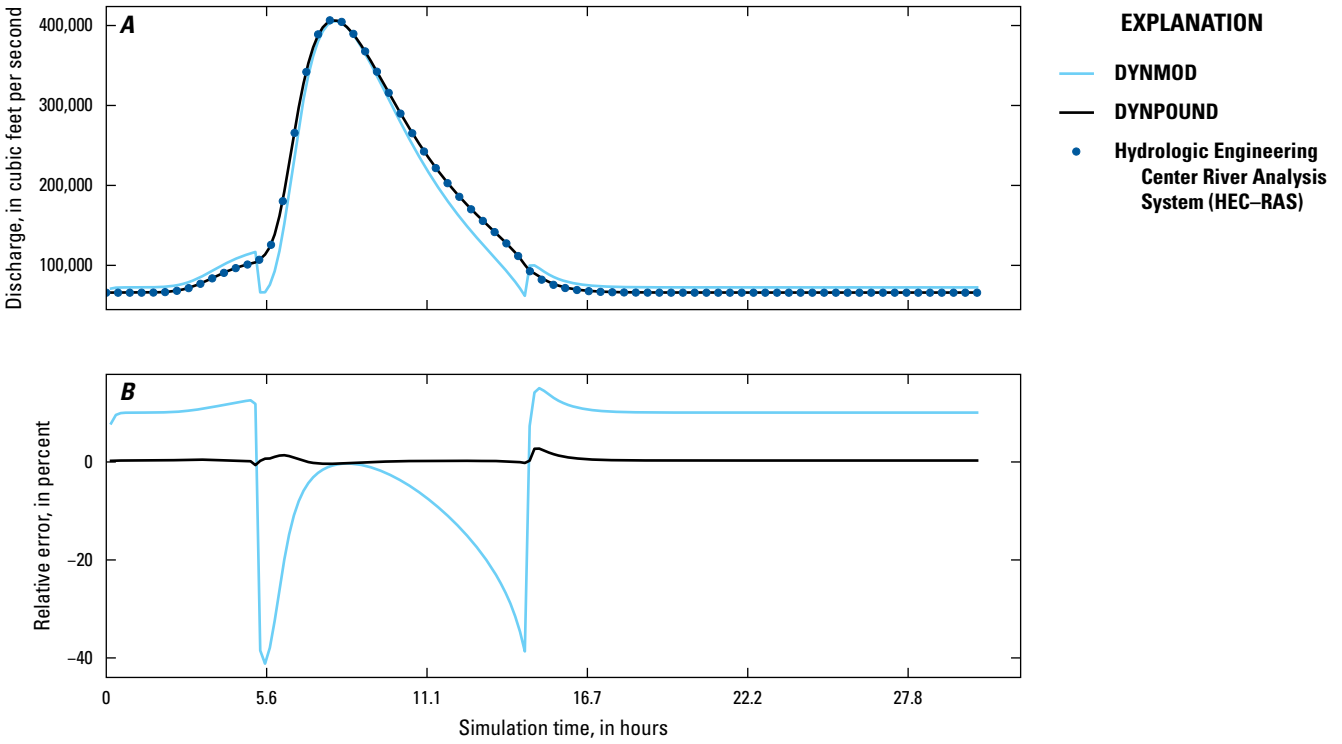

Figure 12. Time series for simulated scenario 3. *A*, Discharge computed with the DYNMOD and DYNPOUND methods; *B*, Percent error of the DYNMOD and DYNPOUND computed discharge time series; DYNMOD, the dynamic rating method that computes discharge from stage for compact channel geometry; DYNPOUND, the newly developed method that solves for discharge in compact and compound channels.

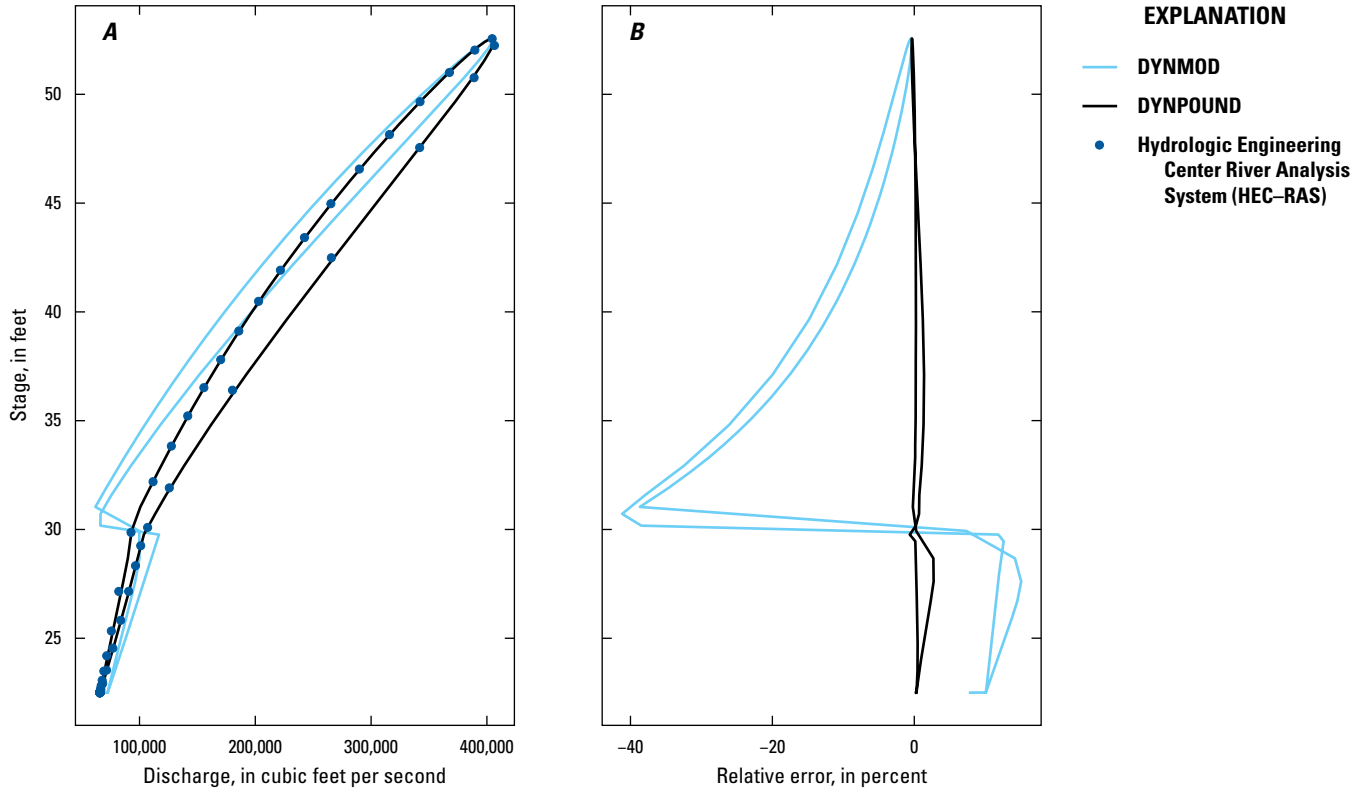

Figure 13. Relation between stage and computed discharge for simulated scenario 3. *A,* DYNMOD and DYNPOUND computed discharge; *B,* Percent error of the DYNMOD and DYNPOUND computed discharge; DYNMOD, the dynamic rating method that computes discharge from stage for compact channel geometry; DYNPOUND, the newly developed method that solves for discharge in compact and compound channels.

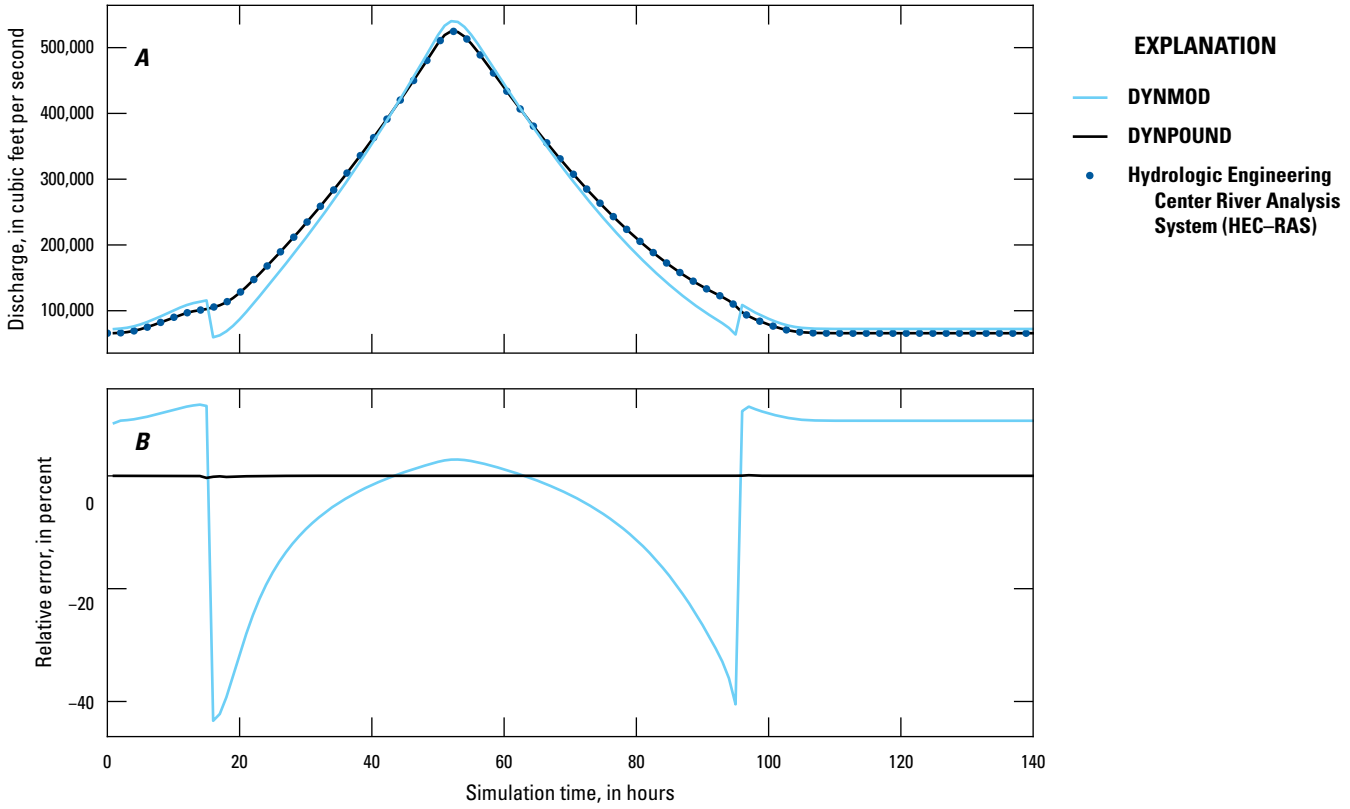

Figure 14. Time series for simulated scenario 4. *A*, Discharge computed with the DYNMOD and DYNPOUND methods; *B*, Percent error of the DYNMOD and DYNPOUND computed discharge time series; DYNMOD, the dynamic rating method that computes discharge from stage for compact channel geometry; DYNPOUND, the newly developed method that solves for discharge in compact and compound channels.

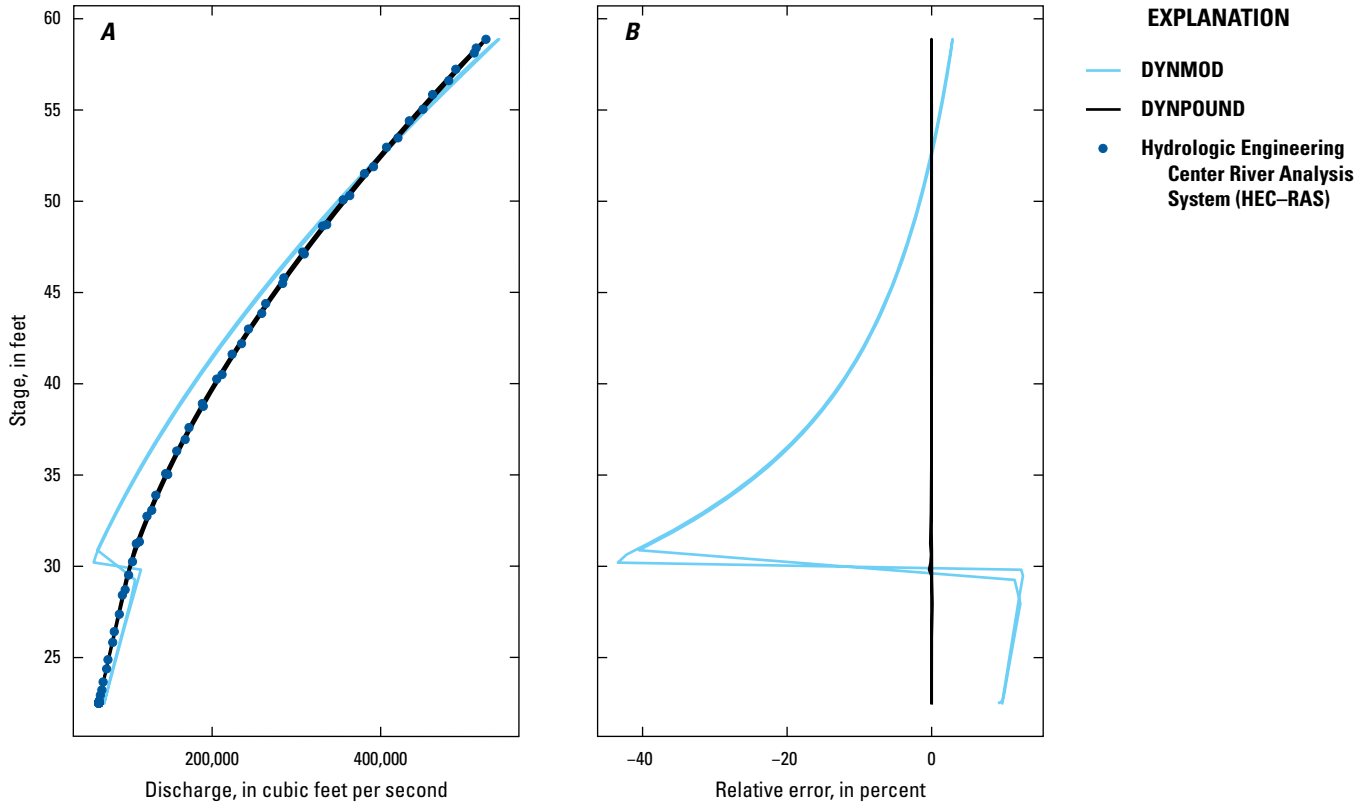

Figure 15. Relation between stage and computed discharge for simulated scenario 4. *A,* DYNMOD and DYNPOUND computed discharge; *B,* Percent error of the DYNMOD and DYNPOUND computed discharge; DYNMOD, the dynamic rating method that computes discharge from stage for compact channel geometry; DYNPOUND, the newly developed method that solves for discharge in compact and compound channels.

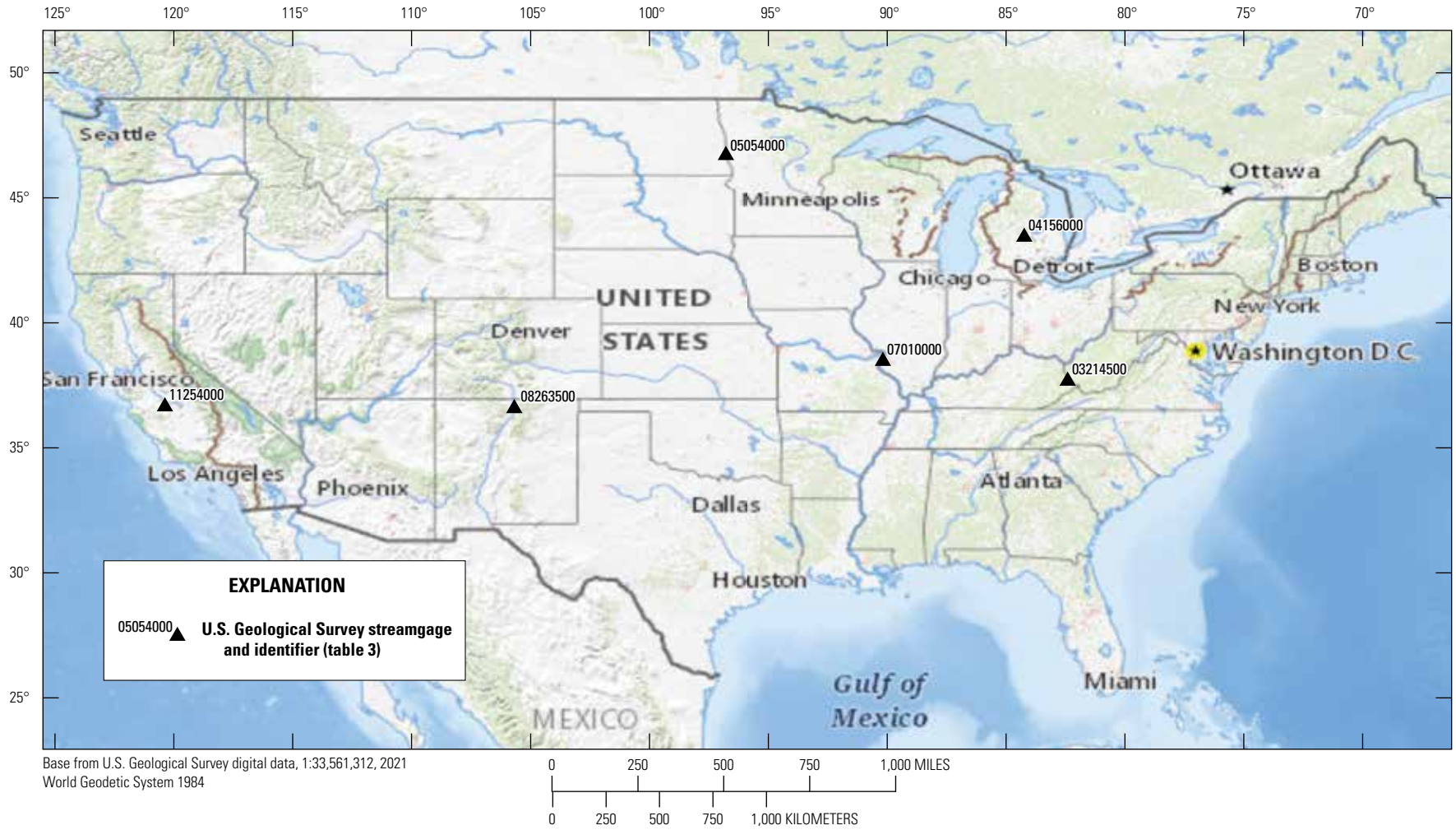

Figure 16. Locations of U.S. Geological Survey streamgage sites used in the evaluation of discharge computed with the dynamic rating methods.

Table 3. Station number and name, drainage area, and slope of the field sites (U.S. Geological Survey, 2020) used in the evaluation of the DYNMOD and DYNPOUND dynamic rating methods.

[mi², square mile; DYNMOD, the dynamic rating method that computes discharge from stage for compact channel geometry; DYNPOUND, the newly developed method that solves for discharge in compact and compound channels]

Station number	Station name	Drainage area (mi²)	Bed slope[1]
03214500	Tug Fork at Kermit, West Virginia	1,277	0.000352
04156000	Tittabawassee River at Midland, Michigan	2,400	0.000139
05054000	Red River of the North at Fargo, North Dakota	6,800	0.000145
07010000	Mississippi River at St. Louis, Missouri	697,000	0.000110
08263500	Rio Grande near Cerro, New Mexico	8,440	0.00360
11254000	San Joaquin River near Mendota, California	3,940	0.000248

[1]Bed slope was calculated using elevation contour and topographical maps and the National Hydrography Dataset (U.S. Geological Survey, 2017; Domanski and others, 2022a)

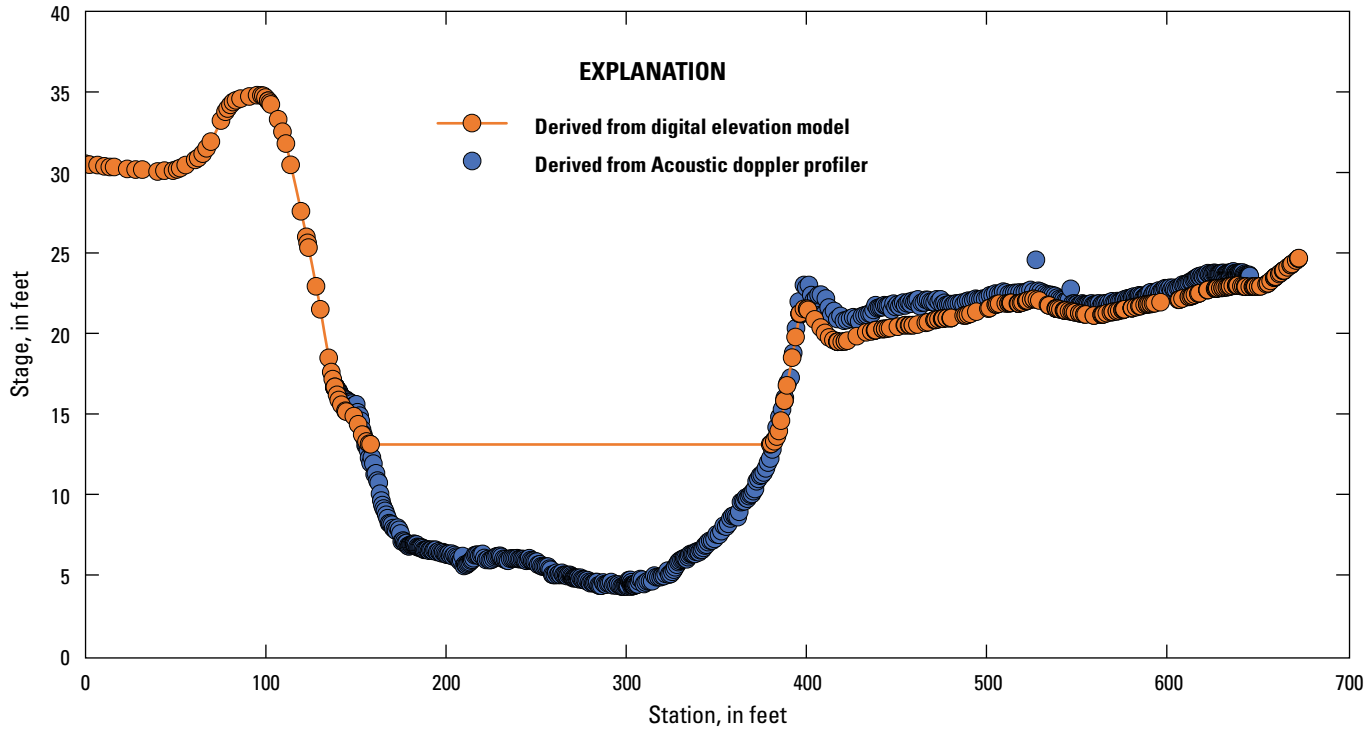

Figure 17. Cross sections derived from acoustic doppler profiler (ADCP) and digital elevation model (DEM) for Tittabawassee River at Midland, Michigan (U.S. Geological Survey station 04156000).

Evaluation Using Field Data

Discrete discharge measurements and stage time series from six USGS streamgages were used for evaluating the DYNMOD and DYNPOUND methods (U.S. Geological Survey, 2020). These streamgage locations represent a variety of geographic locations and geomorphic conditions. The six streamgage sites chosen for evaluation were Tug Fork at Kermit, West Virginia (USGS station 03214500); Tittabawassee River at Midland, Michigan (USGS station 04156000); Red River of the North at Fargo, North Dakota (USGS station 05054000); Mississippi River at St. Louis, Missouri (USGS station 07010000); Rio Grande near Cerro, New Mexico (USGS station 08263500); and San Joaquin River near Mendota, California (USGS station 11254000) (fig. 16, table 3).

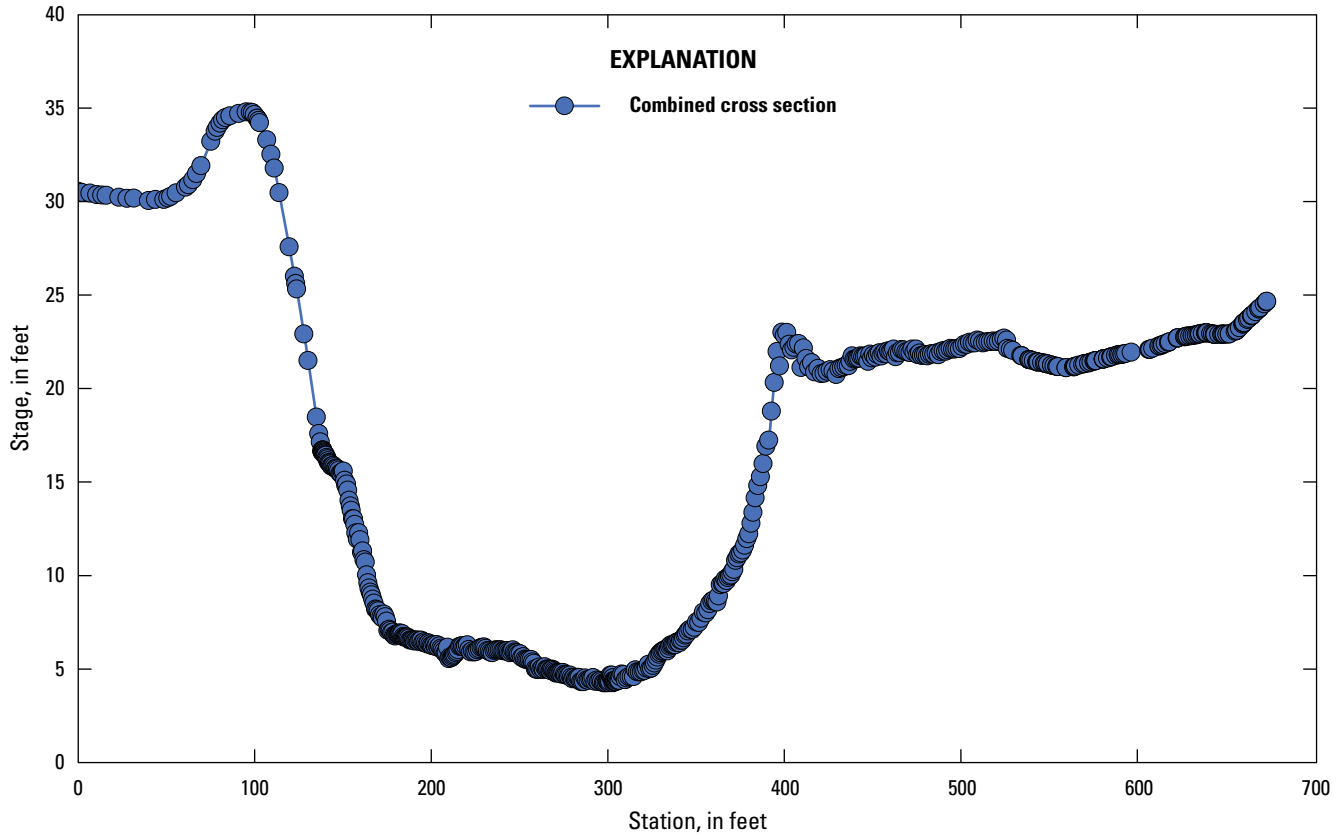

Figure 18. Combined cross section for Tittabawassee River at Midland, Michigan (U.S. Geological Survey station 04156000).

Dataset Development

Site datasets consisted of discharge, stage, and field measurements; cross-section geometry; and bed slope. Discharge, stage, and field measurements were obtained from the National Water Information System (NWIS; U.S. Geological Survey, 2020). Cross-section geometry and bed slope were computed for each site using a combination of acoustic doppler profiler (ADCP) software, AreaComp2 USGS utility (U.S. Geological Survey, 2015), ArcGIS Pro (Esri, 2021), and HEC–RAS (U.S. Army Corps of Engineers, 2016).

Cross-Section Geometry

To obtain cross-section geometry, an ADCP discharge measurement was selected for each site that generally corresponded with a peak flow event. The ADCP measurement was then converted into a "station, depth" coordinate format and imported into AreaComp2. AreaComp2 was used to convert the "station, depth" coordinates to "station, elevation" (in stage datum) coordinates. Next, a digital elevation model (DEM; U.S. Geological Survey, 2017; Michigan State University, 2020; U.S. Department of Agriculture, 2021) was imported into RAS Mapper within HEC–RAS, which was used to generate a "station, elevation" (in stage datum) cross section (fig. 17). This cross section created from the DEM was combined with the cross section created from the ADCP transect to create a cross section that contained the main channel and overbank sections (fig. 18).

The cross section created from the ADCP measurement most accurately represented the channel, and the cross section created from the DEM was used to represent the larger flood plain. In some cases, a measurement was made at a high enough stage to capture some of the flood plain. If this was the case, then "station, elevation" (in stage datum) coordinates from the ADCP measurement superseded the overlapping coordinates from the DEM. Difficulties were encountered in geospatially locating ADCP transects at sites without geolocation data associated with ADCP measurements. If a cross section created from the DEM was used exclusively, it generally lacked accurate channel geometry. If a cross section created from the ADCP was used, it generally lacked flood-plain geometry. In some cases, cross sections with these limitations did not produce accurate results in either of the dynamic rating computation methods. When there was a lack of associated geolocation data for an ADCP measurement, and the location of the cross section was otherwise unable to be located, the cross-section geometry was taken from the DEM exclusively and properties of the channel geometry were estimated.

Bed Slope

Bed slope (S_0) was calculated using elevation contour and historical topographical maps and the National Hydrography Dataset flowline shapefiles (U.S. Geological Survey, 2017; Domanski and others, 2022a). Points were chosen upstream and downstream from each streamgage where an elevation contour line crossed the channel; reach lengths varied depending on available map contours. To compute S_0, the following equation was used:

$$S_0 = \frac{E_{us} - E_{ds}}{L_r} \tag{45}$$

where

S_0 is bed slope, in feet per feet;
E_{us} is upstream elevation, in feet;
E_{ds} is downstream elevation, in feet; and
L_r is length of reach, in feet.

Evaluation

Discharge time series were computed with the dynamic rating methods at gaged field sites where cross-section geometry was created and real-time stage and discharge data were being collected. Discharge time series were computed at six streamgage sites in California, Michigan, Missouri, New Mexico, North Dakota, and West Virginia.

For all sites, an event was chosen for computing the r value that typically was an isolated flood wave with a moderate peak stage and discharge. The stage at the time immediately prior to the onset of the flood event was inserted to equation 18 as h_0. The peak stage from this event is h_p in equation 18. The time of the peak minus the time of occurrence of h_0 is τ in equation 18.

Subsections were added to the cross section for each site based on the need to (i) develop a smooth conveyance and stage relation, (ii) add regions where transitions in roughness can be made in the flood plain, (iii) remove those areas of the cross section that do not contribute to the momentum of the flow, and (iv) allow for computation of the non-uniform velocity distribution coefficient.

To determine the smoothness of the conveyance/stage relation, conveyance was plotted against stage and visually analyzed. If an abrupt change in slope of the relation was observed, the cross section was analyzed for sudden changes in geometry. Existing subsections that contained sudden changes in geometry were split into two subsections by inserting a split where the changes take place.

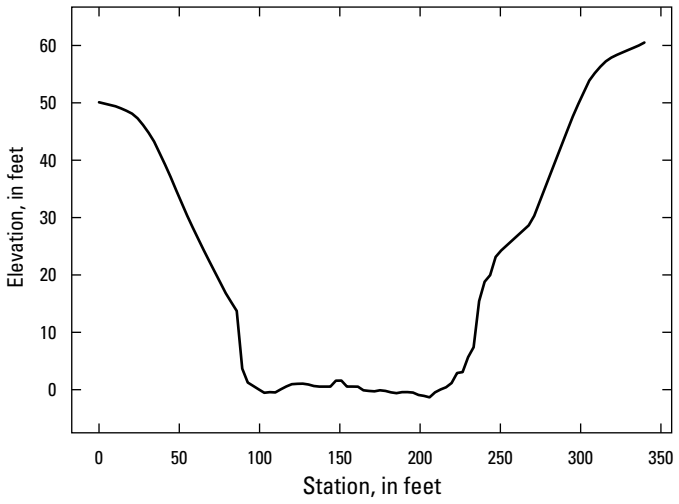

Figure 19. Cross section used in the computation of the discharge time series for the Tug Fork at Kermit, West Virginia (U.S. Geological Survey station 03214500). Elevation is referenced to 574.07 feet above North American Vertical Datum of 1988.

Table 4. Calibration results for the DYNMOD and DYNPOUND ratings at the Tug Fork at Kermit, West Virginia (U.S. Geological Survey station 03214500).

[Observed discharge data from U.S. Geological Survey (2020). MM, month; DD, day; YYYY, year; UTC, Universal Time Coordinated; ft³/s, cubic feet per second; DYNMOD, the dynamic rating method that computes discharge from stage for compact channel geometry; SLE, squared logarithmic error; DYNPOUND, the newly developed method that solves for discharge in compact and compound channels; --, not applicable]

Measurement date (MM/DD/YYYY)	Measurement time (UTC)	Observed discharge (ft³/s)	DYNMOD discharge (ft³/s)	DYNMOD error (percent)	DYNMOD SLE	DYNPOUND discharge (ft³/s)	DYNPOUND error (percent)	DYNPOUND SLE
11/3/2015	19:48	344	394	14.6	1.84×10^{-2}	390	13.6	1.58×10^{-2}
1/13/2016	19:22	641	643	0.444	9.70×10^{-6}	636	−0.662	6.13×10^{-5}
3/22/2016	17:48	1,090	1,053	−3.34	1.19×10^{-3}	1,036	−4.91	2.58×10^{-3}
5/12/2016	19:11	7,540	7,636	1.28	1.60×10^{-4}	7,141	−5.28	2.96×10^{-3}
7/21/2016	18:53	805	817	1.53	2.19×10^{-4}	806	0.167	1.54×10^{-6}
9/19/2016	17:40	688	676	−1.71	3.10×10^{-4}	668	−2.82	8.70×10^{-4}
Mean	--	--	--	2.13	3.38×10^{-3}	--	0.0158	3.70×10^{-3}

A full water year of stage and discharge time series was chosen for calibrating the method at each site (a water year is defined as the 12-month period, October 1 through September 30, and is designated by calendar year in which it ends). At least five field measurements were compared for calibration at each of the six streamgages for which results are discussed. To calibrate the computations for a site, the Manning's *n* values of the cross section were modified, and sometimes subsectioning of the cross section was implemented so the computed measurement would match the field measurement. The bed slope, *r* value, and cross-section geometry were considered fixed values during the calibration.

After the calibration for the site was completed, a different period of time in the record was selected to evaluate the method. For each site, the evaluation time period is after the calibration time period, which contains a substantial amount of field measurements and a wide range of observed discharge values. Discharge values from field measurements were then compared to dynamic rating computed discharge at the corresponding times.

In some cases, stage data were missing from the observed time series. As long as the period of missing data was short, the missing stage data were estimated through linear interpolation.

Tug Fork at Kermit, West Virginia

The USGS streamgage Tug Fork at Kermit, West Virginia (USGS station 03214500) represents an upstream basin of 1,277 square miles (mi^2). The computed bed slope for the site is 0.000352 (table 3). The *r* value, computed from the event with a peak stage of 24.35 feet occurring at 1:15 (Universal Time Coordinated [UTC]) on April 25, 2017 (U.S. Geological Survey, 2020), is 37.2. The cross section used in the computation of the time series is shown in figure 19.

Six discharge measurements from the 2016 water year were used for calibration. The stage time series for the 2016 water year was used to compute discharge (U.S. Geological Survey, 2020). No subdivision of the cross section was used in the DYNMOD calibration. For DYNPOUND, although subdivision of the cross section can be accommodated, the cross section does not meet criteria for this site (Davidian, 1984). A Manning's *n* value of 0.044 was used for the full cross section for both methods.

The MSLE for the DYNMOD calibration was 3.38×10^{-3}, and the MSLE for the DYNPOUND calibration was 3.70×10^{-3}. The mean percent error of the DYNMOD calibration was 2.13 percent, and the mean percent error of the DYNPOUND calibration was 0.0158 percent (table 4).

For evaluation of the ratings for the USGS streamgage Tug Fork at Kermit, West Virginia, discharge was computed for the time period between February 1 and March 1, 2018, which also included five field measurements (fig. 20). Both methods (DYNMOD and DYNPOUND) capture hysteresis in the stage/discharge relation for the computed event, whereas the USGS-computed discharge is singled-valued and failed to capture hysteresis (fig. 21). A comparison of the observed and computed discharge for the time period indicates the results of both dynamic rating methods were biased high when compared to the field measurements, with a mean error of 13.4 percent for DYNMOD and 6.38 percent for DYNPOUND. The MSLE was 3.14×10^{-2} and 1.77×10^{-2} for the DYNMOD and DYNPOUND computed time series, respectively (table 5).

Tittabawassee River at Midland, Michigan

The USGS streamgage Tittabawassee River at Midland, Michigan (USGS station 04156000) represents an area of 2,400 mi^2. The computed bed slope for the site is 0.000139 (table 3). The *r* value was computed as 18.1 using the event with a peak stage of 22.16 feet occurring at 12:30 (UTC) on

Table 5. Discharge computed for an event-based time series at the Tug Fork at Kermit, West Virginia (U.S. Geological Survey station 03214500) with the DYNMOD and DYNPOUND methods and the associated error.

[Observed discharge data from U.S. Geological Survey (2020).MM, month; DD, day; YYYY, year; UTC, Universal Time Coordinated; ft^3/s, cubic feet per second; DYNMOD, the dynamic rating method that computes discharge from stage for compact channel geometry; SLE, squared logarithmic error; DYNPOUND, the newly developed method that solves for discharge in compact and compound channels; --, not applicable]

Measurement date (MM/DD/YYYY)	Measurement time (UTC)	Observed discharge (ft^3/s)	DYNMOD discharge (ft^3/s)	DYNMOD error (percent)	DYNMOD SLE	DYNPOUND discharge (ft^3/s)	DYNPOUND error (percent)	DYNPOUND SLE
2/5/2018	18:51	3,030	2,814	−7.10	5.47×10^{-3}	2,725	−10.0	1.13×10^{-2}
2/11/2018	19:24	27,600	30,932	12.1	1.30×10^{-2}	28,975	4.98	2.36×10^{-3}
2/11/2018	20:52	29,100	33,620	15.5	2.08×10^{-2}	31,394	7.88	5.76×10^{-3}
2/11/2018	22:21	34,400	36,496	6.09	3.50×10^{-3}	34,040	−1.04	1.11×10^{-4}
2/12/2018	20:59	22,100	30,995	40.2	1.14×10^{-1}	28,746	30.1	6.91×10^{-2}
Mean	--	--	--	13.4	3.14×10^{-2}	--	6.38	1.77×10^{-2}

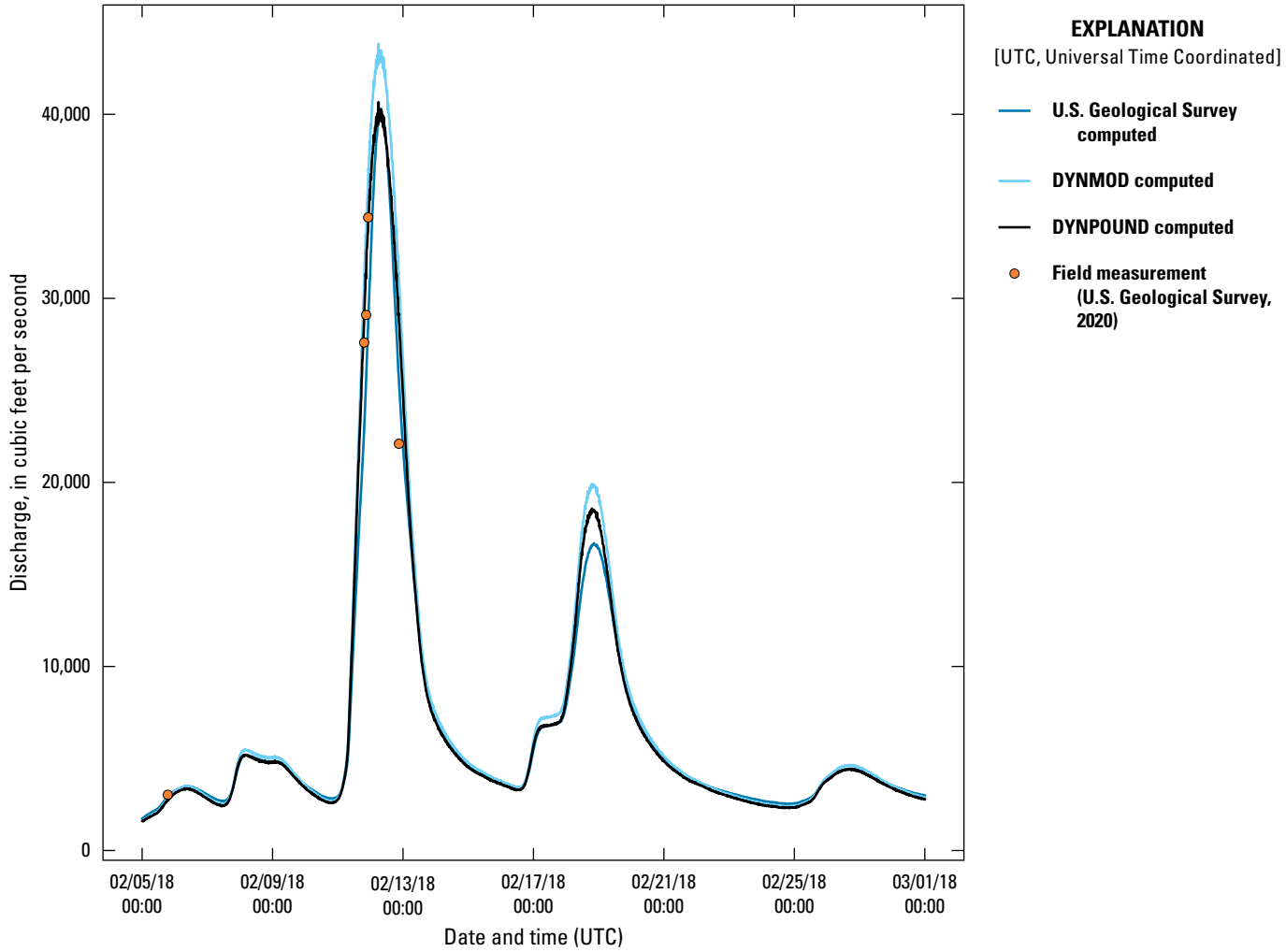

Figure 20. Discharge time series computed with the DYNMOD and DYNPOUND methods shown with the U.S. Geological Survey-computed discharge time series and field measurements made at Tug Fork at Kermit, West Virginia (U.S. Geological Survey station 03214500).

April 11, 2015 (U.S. Geological Survey, 2020). The cross section used in the computation of the time series is shown in figure 22.

Nine discharge measurements collected during the 2017 water year were used for calibration (fig. 23). The stage time series from the 2017 water year was used to compute discharge. The DYNMOD method failed to compute discharge during the entire period of calibration so the calibration results were not quantified. The channel cross section was split into three subsections for the DYNPOUND computation with subsection stations at 90 and 401 feet (fig. 22). The leftmost subsection of the cross section, which was assigned a Manning's *n* value of 0.035, was used in the computation of the hydraulic properties of the cross section for stages above 35 feet. The rightmost subsection, assigned a Manning's *n* value of 0.015, was used for the right bank flood-plain area at stages above 22.9 feet. When stages were above the maximum elevation of the rightmost subsection, a vertical wall with friction was extended from the rightmost station to the water surface. The middle subsection, which contains the geometry of the main channel and is assigned a Manning's *n* value of 0.035, is always used in the computation of hydraulic properties. The calibration results for the DYNPOUND computation indicate the MSLE was 3.42×10^{-2} and the mean percent error was −2.36 percent (table 6).

Discharge measurements and discharge time series computed with DYNPOUND and the simple rating method were evaluated for the time period between May 1 and June 30, 2020 (fig. 23). The peak of the time period is an extreme event for the site owing to a dam break upstream. The stage hydrograph reached a stage that was above the stage values defined by the cross-section geometry (fig. 24).

The discharge values computed with DYNPOUND were compared to three field measurements and indicated the DYNPOUND method had a mean percent error of 5.58 percent and an MSLE of 3.64×10^{-3} (table 7). The dynamic rating method

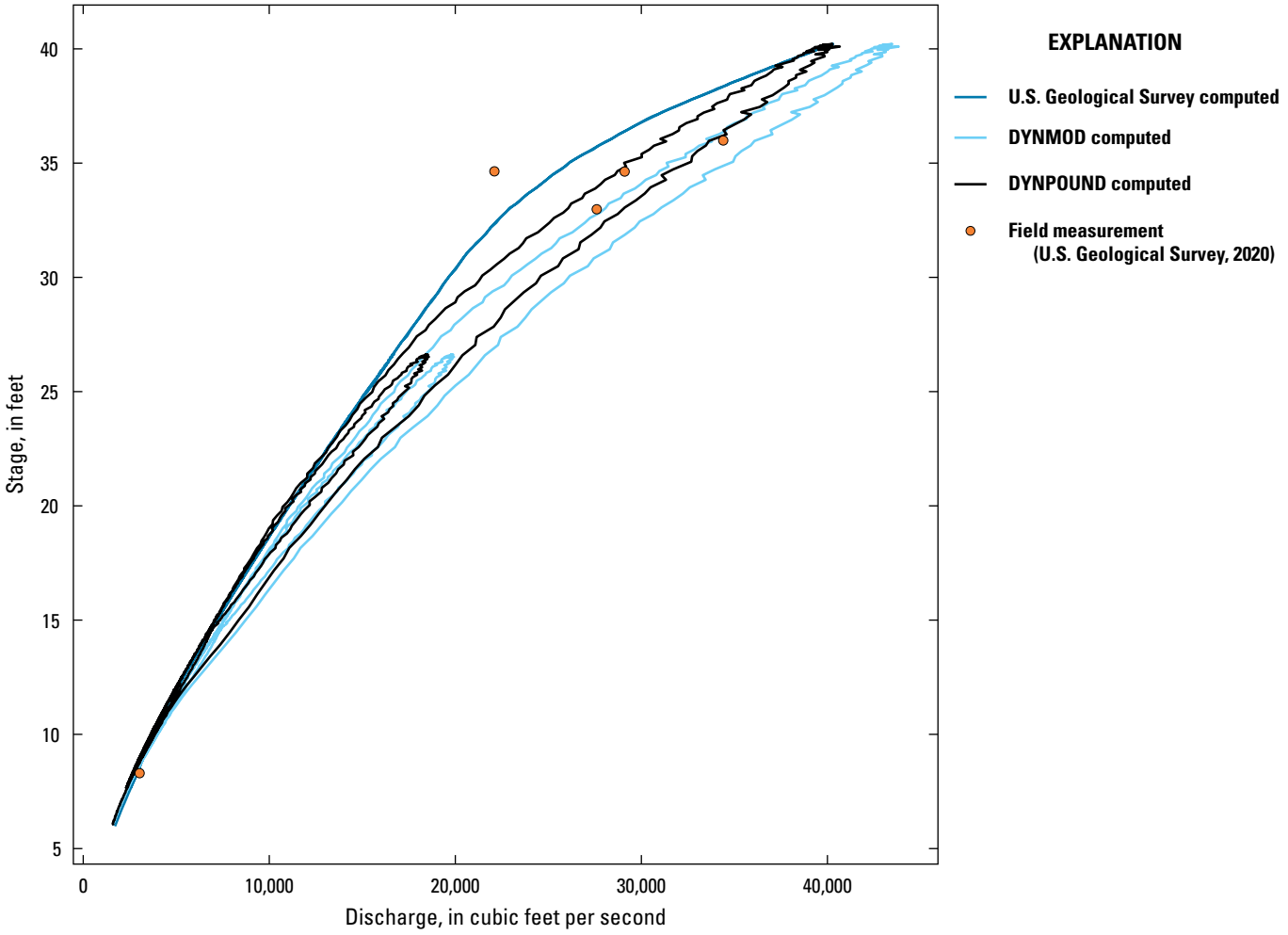

Figure 21. Stage/discharge relation of the discharge computed with the DYNMOD and DYNPOUND methods shown with U.S. Geological Survey-computed discharge and field measurements made at Tug Fork at Kermit, West Virginia (U.S. Geological Survey station 03214500). Elevation is referenced to 574.07 feet above North American Vertical Datum of 1988.

captured hysteresis in the stage/discharge relation, whereas the USGS-computed discharge did not (fig. 24). The stage/discharge relation computed with DYNPOUND shows an oscillation between high and low discharges near the peak stage of the time series, which may be due to the poor definition of the cross-section geometry under the extreme flow conditions. An improvement to the computation of discharge for this site would be to include a better definition of the channel geometry at high stages.

Red River of the North at Fargo, North Dakota

The USGS streamgage Red River of the North at Fargo, North Dakota (U.S. Geological Survey station 05054000) represents a basin draining an area of 6,800 mi^2. The computed slope for the site is 0.000145 (table 3). The *r* value, computed from the event with a peak stage of 27.85 feet occurring at 23:30 (UTC) on June 23, 2014 (U.S. Geological Survey, 2020), is computed as 27.4. The cross section used in the computation of the time series is shown in figure 25.

Twelve field measurements collected during the 2019 water year were used for calibration. The stage time series from the 2019 water year was used to compute discharge. The DYNMOD method failed to compute discharge during the entire period of calibration, so the calibration results for the DYNMOD method are not quantified. The cross section was split into four subsections for the DYNPOUND computation. Subsection stations are 620, 875, and 1,090 feet. The calibrated Manning's *n* values for the subsections, from left to right, are 0.035, 0.065, 0.06, and 0.065. The MSLE for the DYNPOUND calibration was 4.57×10^{-1} and the mean percent error was 61.9 percent (table 8).

A discharge time series was computed with DYNPOUND for the time period between March 16 and May 5, 2020, and used to evaluate the generated rating with six field measurements collected during this period (fig. 26). The

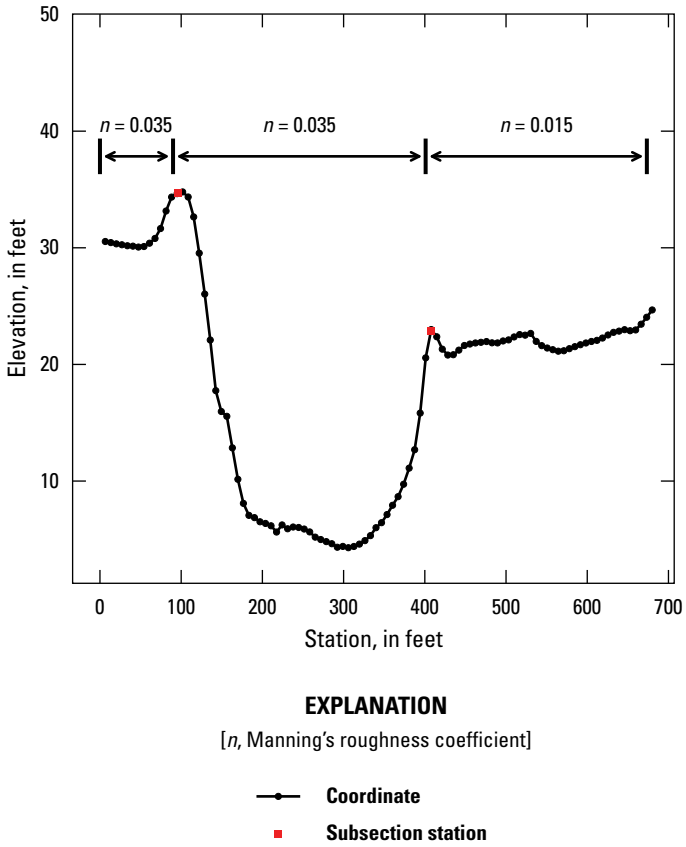

Figure 22. Cross section used in the computation of the discharge time series for the Tittabawassee River at Midland, Michigan (U.S. Geological Survey station 04156000). Elevation is referenced to 579.47 feet above North American Vertical Datum of 1988.

Table 6. Calibration results for the DYNPOUND rating at the Tittabawassee River at Midland, Michigan (U.S. Geological Survey station 04156000).

[Observed discharge data from U.S. Geological Survey (2020). MM, month; DD, day; YYYY, year; UTC, Universal Time Coordinated; DYNPOUND, the newly developed method that solves for discharge in compact and compound channels; ft^3/s, cubic feet per second; SLE, squared logarithmic error; --, not applicable]

Measurement date (MM/DD/YYYY)	Measurement time (UTC)	Observed discharge (ft^3/s)	DYNPOUND discharge (ft^3/s)	DYNPOUND error (percent)	DYNPOUND SLE
10/12/2016	15:22	905	1,097	21.3	3.70×10^{-2}
12/1/2016	18:14	2,960	2,292	−22.5	6.54×10^{-2}
1/27/2017	19:03	6,020	4,502	−25.2	8.44×10^{-2}
3/16/2017	17:15	2,290	1,843	−19.5	4.72×10^{-2}
5/10/2017	15:51	2,040	1,774	−13.0	1.95×10^{-2}
6/24/2017	15:12	37,700	39,831	5.65	3.02×10^{-3}
6/24/2017	16:58	38,800	40,035	3.19	9.82×10^{-4}
6/26/2017	15:31	19,100	19,871	4.04	1.57×10^{-3}
8/25/2017	11:40	765	954	24.8	4.87×10^{-2}
Mean	--	--	--	−2.36	3.42×10^{-2}

Table 7. Discharge computed with the DYNPOUND method and associated error for an event-based time series at Tittabawassee River at Midland, Michigan (U.S. Geological Survey station 04156000).

[Observed discharge data from U.S. Geological Survey (2020). MM, month; DD, day; YYYY, year; UTC, Universal Time Coordinated; DYNPOUND, the newly developed method that solves for discharge in compact and compound channels; ft^3/s, cubic feet per second; SLE, squared logarithmic error; --, not applicable]

Measurement date (MM/DD/YYYY)	Measurement time (UTC)	Observed discharge (ft^3/s)	DYNPOUND discharge (ft^3/s)	DYNPOUND error (percent)	DYNPOUND SLE
5/20/2020	17:48	51,500	53,537	3.96	1.50×10^{-3}
5/20/2020	19:31	49,900	51,475	3.16	9.66×10^{-4}
5/21/2020	19:18	30,100	32,996	9.62	8.44×10^{-3}
Mean	--	--	--	5.58	3.64×10^{-3}

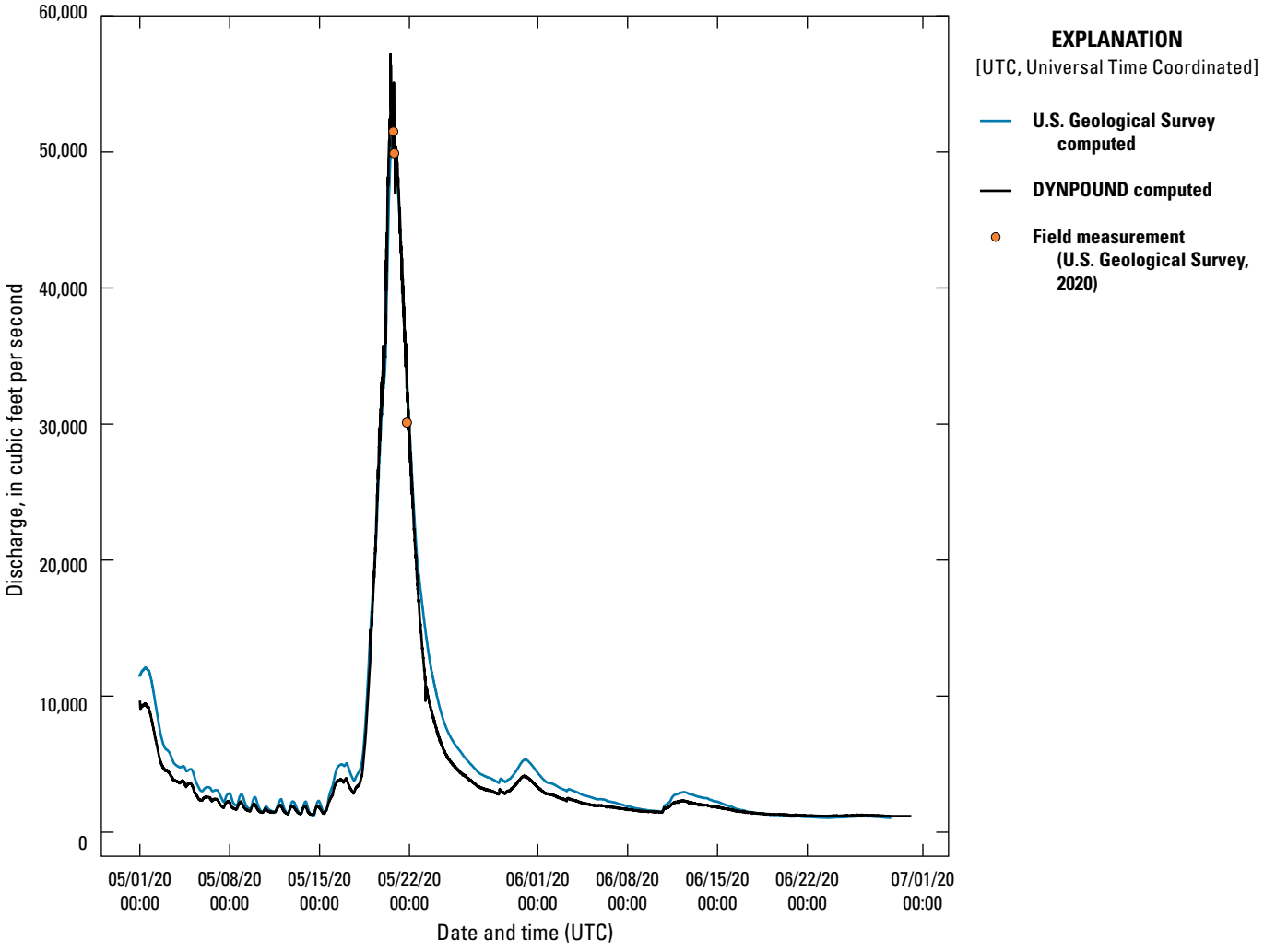

Figure 23. Discharge time series computed with the DYNPOUND method shown with the rated discharge time series and field measurements made at Tittabawassee River at Midland, Michigan (U.S. Geological Survey station 04156000).

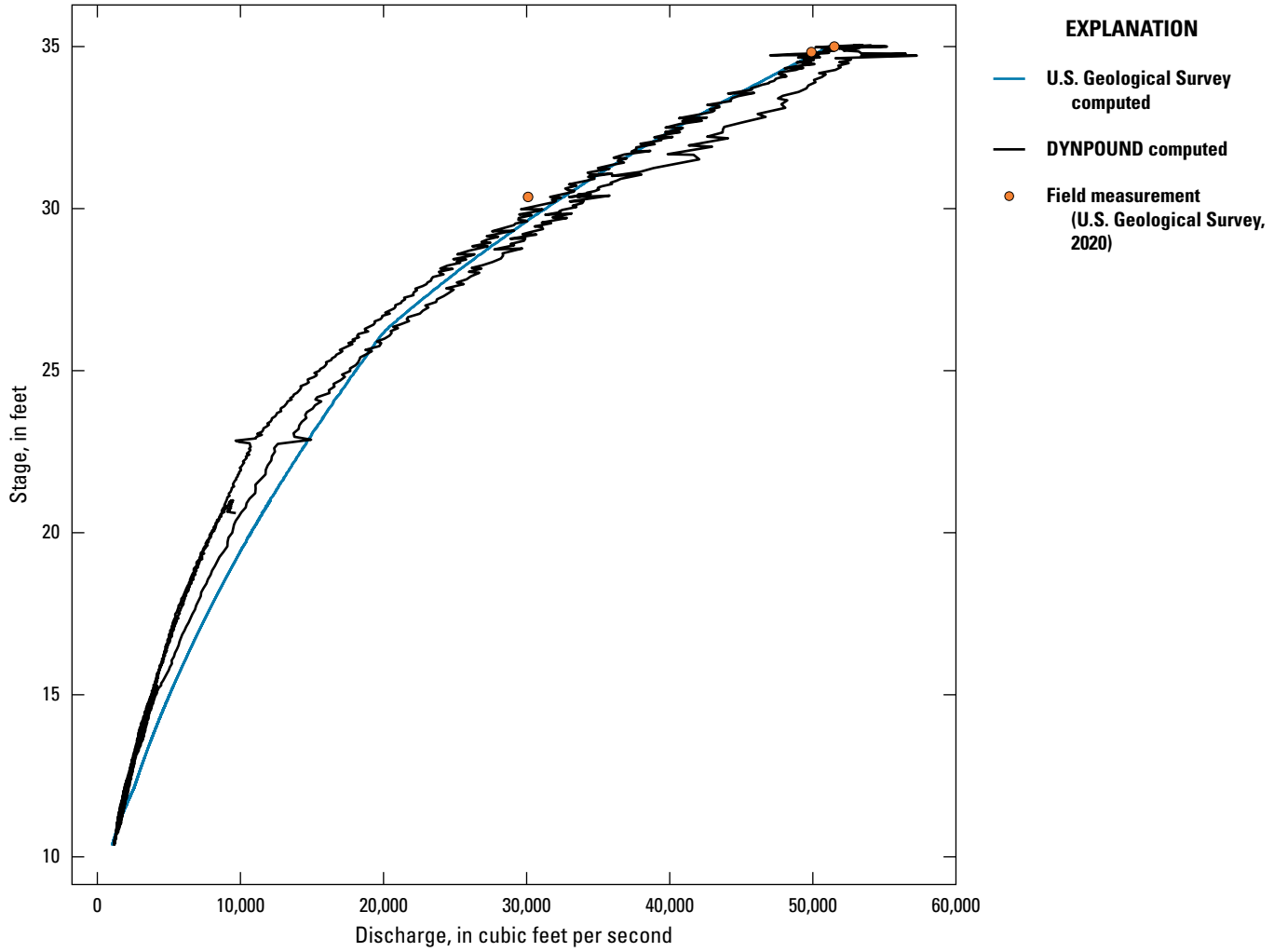

Figure 24. Stage/discharge relation of the discharge computed with the DYNPOUND method shown with U.S. Geological Survey-computed discharge and field measurements made at the Tittabawassee River at Midland, Michigan (U.S. Geological Survey station 03214500).

stage/discharge relation for the computed event is shown in figure 27. During this time period, six field measurements are available for comparison. The mean percent error of the DYNPOUND computed discharge was −19.9 percent (table 9) and the MSLE was 7.23×10^{-2}. As shown graphically in the time series and stage/discharge plots, and quantitatively by the mean percent error, the DYNPOUND computed discharge is substantially lower than the observed discharge during the time period.

Mississippi River at St. Louis, Missouri

The USGS streamgage Mississippi River at St. Louis, Missouri (USGS station 07010000) represents a basin draining an area of 697,000 mi^2. The bed slope for the site is 0.000110 (table 3). An *r* value of 13.5 was computed using the event with a peak stage of 24.8 feet occurring at 14:00 (UTC) on March 13, 2013 (U.S. Geological Survey, 2020). The cross section used in the computation of the discharge time series is shown in figure 28.

Eleven discharge measurements collected during the 2014 water year were used for calibration of the dynamic ratings for the Mississippi River at St. Louis, Missouri, streamgage. The stage time series from the 2014 water year was used to compute discharge. The roughness coefficient used in the DYNMOD computations varied with stage (fig. 29), whereas a constant Manning's *n* value of 0.044 was used in the DYNPOUND rating. No subdivision of the cross section for this site was made in the computation of discharge with the DYNPOUND method.

For the DYNMOD calibration, the MSLE was 2.19×10^{-3} and the mean percent error was 1.82 percent. For the DYNPOUND calibration, the MSLE was 3.02×10^{-2} and the mean percent error was 1.42 percent (table 10).

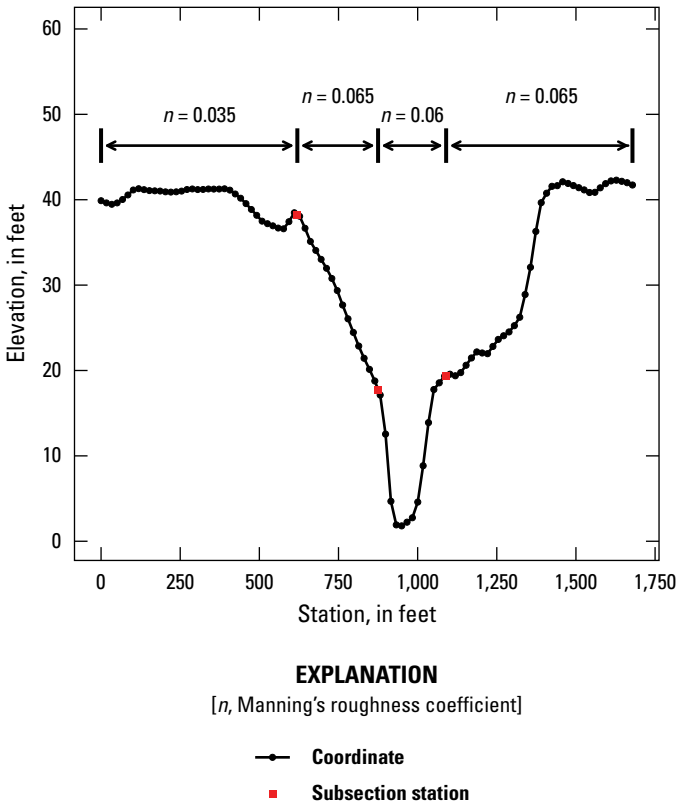

Figure 25. Cross section used in the computation of the discharge time series for the Red River of the North at Fargo, North Dakota (U.S. Geological Survey station 05054000). Elevation is referenced to 862.88 feet above North American Vertical Datum of 1988.

To evaluate the dynamic rating methods for this site, discharge for the time period between June 1 and August 15, 2015, was computed and observed, and computed discharge values were compared for 68 field discharge measurements. The mean percent error for the discharge computed with the DYNMOD method was 2.18 percent and the mean percent error for the DYNPOUND method was −22.1 percent (table 11). The MSLE for the DYNMOD method results was 2.76×10^{-3} and the 7.11×10^{-2} for the DYNPOUND results. The discharge computed with the DYNPOUND method was considerably lower than the observed discharge, whereas the DYNMOD computed discharge matches much better with the observed discharge values (figs. 30 and 31).

Although the mean percent error of the calibration for the DYNPOUND method shows low bias during the water year of calibration, the magnitude of discharge observed during the event time series was greater than the DYNPOUND computed discharge. It was possible to calibrate the DYNPOUND method by minimizing the MSLE for water year 2015, and the calibration resulted in a small mean percent error, but the magnitude of the largest percent error was 29.8 percent. The current implementation of the DYNPOUND does not allow for a stage/roughness relation to be specified in the computation of discharge. Because of this, the calibration of the DYNPOUND method resulted in low bias but large error during a full water year. Large discharge values are observed during the event time series used in the evaluation of the dynamic rating methods, so large errors occur in the discharge computed with the DYNPOUND method. Implementation of the feature that allows for a specification of a stage/roughness relation, as is possible with the DYNMOD method, may provide the ability to refine the DYNPOUND calibration and reduce the errors in the computed time series.

Rio Grande Near Cerro, New Mexico

The USGS streamgage Rio Grande near Cerro, New Mexico (USGS station 08263500) represents a basin draining an area of 8,440 mi^2. The bed slope for the site is computed as 0.00360 (table 3). An r value of 2,790 was computed using the event with a peak stage of 7.76 feet occurring at 15:45 (UTC) on June 20, 2015 (U.S. Geological Survey, 2020). The r values are expected to fall within 10 and 100 (Fread, 1973). The computed r value for this site is an order of magnitude larger than the largest expected value. Further investigation would be helpful to determine the cause of the high r value for this site.

Seven field measurements of discharge collected during the 2015 water year were used for calibration. The stage time series from the 2015 water year was used to compute discharge. No subdivision of the cross section (fig. 32) takes place in the computation of the hydraulic properties for either dynamic rating method. A Manning's n value of 0.120 was used for the full cross section for both methods. The calibrated Manning's n value was much higher than expected, and the high Manning's n value may be compensating for the high r value or other phenomena not adequately captured in the rating.

The MSLE and mean percent error for the DYNMOD method were 9.77×10^{-3} and −2.95 percent, respectively. The calibration results for the DYNPOUND method were 1.02×10^{-2} and −3.86 percent, respectively (table 12).

The time period between April 1 and August 5, 2019, was used to evaluate the discharge computed with the dynamic rating methods for this site. Although only two measurements were made during the event time period, both dynamic rating methods were biased high (figs. 33 and 34). The mean percent error of the DYNMOD results is 11.05 percent, and the mean percent error of the DYNPOUND results is 9.40 percent. The MSLE of the DYNMOD results is 1.09×10^{-2} and the MSLE for the DYNMOD results is 7.96×10^{-3} (table 13).

San Joaquin River Near Mendota, California

The USGS streamgage San Joaquin River near Mendota, California (U.S. Geological Survey station 11254000) represents a basin draining an area of 3,940 mi^2. The computed slope for the site is 0.000248 (table 3). An r value of 158 was computed from the event with a peak stage of 5.46 feet

Table 8. Calibration results for the DYNPOUND rating at the Red River of the North at Fargo, North Dakota (U.S. Geological Survey station 05054000).

[Observed discharge data from U.S. Geological Survey (2020). MM, month; DD, day; YYYY, year; UTC, Universal Time Coordinated; ft³/s, cubic feet per second; DYNPOUND, the newly developed method that solves for discharge in compact and compound channels; SLE, Squared logarithmic error; --, not applicable]

Measurement date (MM/DD/YYYY)	Measurement time (UTC)	Observed discharge (ft³/s)	DYNPOUND discharge (ft³/s)	DYNPOUND error (percent)	DYNPOUND SLE
11/2/2018	16:13	434	1,586	266	1.68
1/23/2019	18:00	442	1,621	267	1.69
3/5/2019	23:15	432	1,621	275	1.75
4/2/2019	22:28	7,340	4,655	−36.6	2.07×10^{-1}
4/5/2019	17:42	15,500	14,683	−5.27	2.93×10^{-3}
4/6/2019	18:23	17,200	18,066	5.04	2.41×10^{-3}
4/7/2019	18:50	19,500	19,759	1.33	1.74×10^{-4}
4/8/2019	19:49	19,200	20,329	5.88	3.26×10^{-3}
4/15/2019	23:04	11,400	11,952	4.84	2.24×10^{-3}
4/23/2019	21:32	13,000	13,318	2.45	5.84×10^{-4}
6/11/2019	17:27	3,390	2,332	−31.2	1.40×10^{-1}
7/23/2019	15:34	2,450	2,179	−11.1	1.37×10^{-2}
Mean	--	--	--	61.9	4.57×10^{-1}

Table 9. Discharge computed with the DYNPOUND method and associated error for an event-based time series at the Red River of the North at Fargo, North Dakota (U.S. Geological Survey station 05054000).

[Observed discharge data from U.S. Geological Survey (2020). MM, month; DD, day; YYYY, year; UTC, Universal Time Coordinated; ft³/s, cubic feet per second; DYNPOUND, the newly developed method that solves for discharge in compact and compound channels; SLE, Squared logarithmic error; --, not applicable]

Measurement date (MM/DD/YYYY)	Measurement time (UTC)	Observed discharge (ft³/s)	DYNPOUND discharge (ft³/s)	DYNPOUND error (percent)	DYNPOUND SLE
3/26/2020	17:32	4,250	2,944	−30.7	1.35×10^{-1}
3/31/2020	18:03	11,700	9,692	−17.2	3.55×10^{-2}
4/4/2020	17:36	7,750	7,630	−1.54	2.44×10^{-4}
4/9/2020	14:51	10,300	9,208	−10.6	1.26×10^{-2}
4/15/2020	16:58	5,990	4,232	−29.3	1.21×10^{-1}
5/1/2020	15:44	3,400	2,370	−30.3	1.30×10^{-1}
Mean	--	--	--	−19.9	7.23×10^{-2}

occurring at 12:30 (UTC) on February 22, 2015 (U.S. Geological Survey, 2020). The cross section used in the computation of the time series is shown in figure 35.

Nine discharge measurements collected during the 2017 water year were used for calibration. The stage time series from the 2017 water year was used to compute discharge. The DYNMOD method failed to compute discharge the entire period of calibration, so the calibration results for the DYNMOD method are not quantified. The cross section for the DYNPOUND analyses was subdivided into three subsections, with the subsection between 540 and 700 feet being the only subsection that is used in the computation of discharge. A Manning's *n* value of 0.035 was assigned to this subsection. The MSLE for the DYNPOUND calibration was 1.25 and the mean percent error was 307 percent (table 14). A measurement with an extremely high error of 2,530 percent occurred on January 10, 2017, at 20:48 UTC. The observed discharge at this time was 0.67 ft³/s, and the DYNPOUND computed discharge was 17 ft³/s.

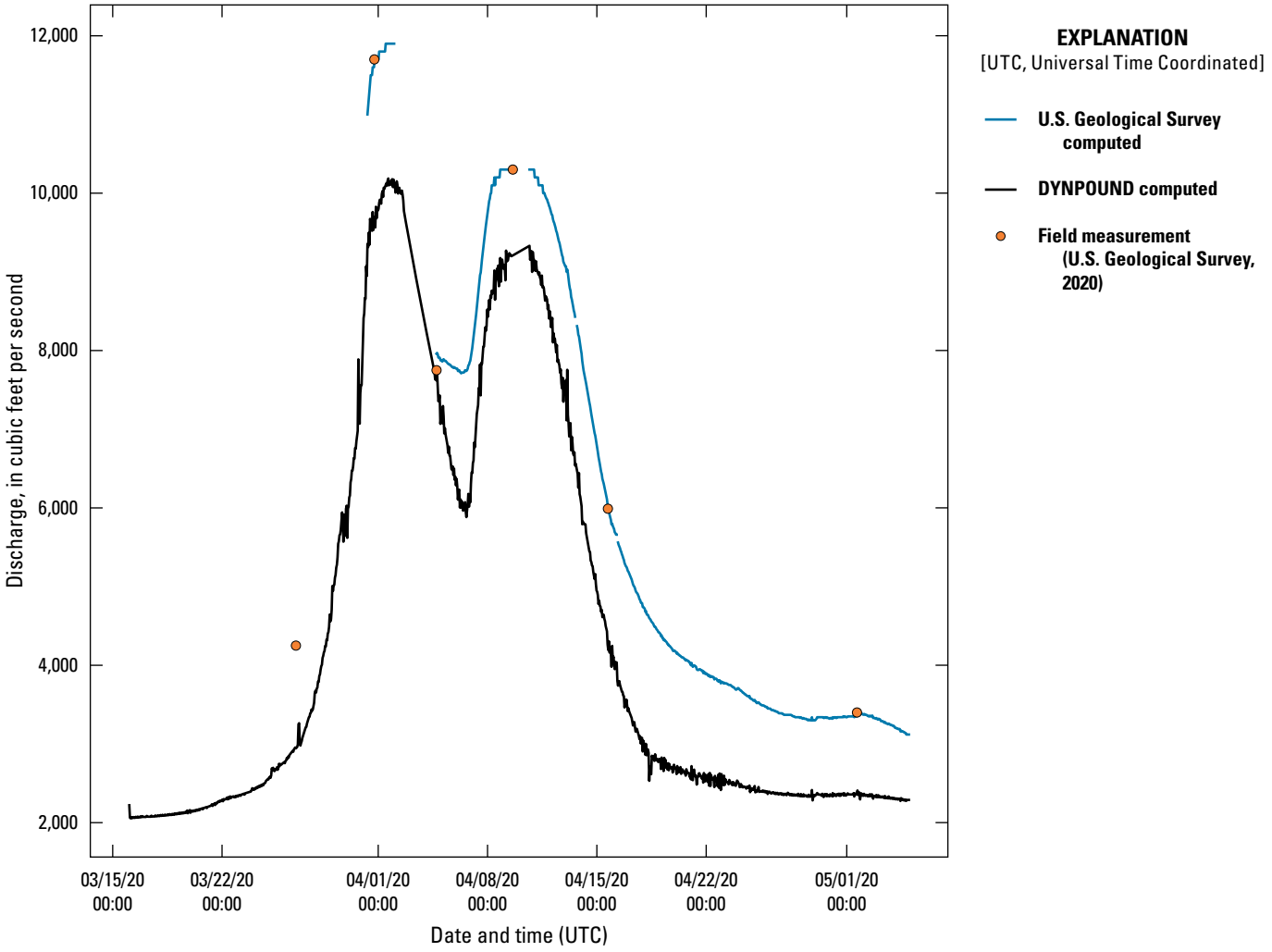

Figure 26. Discharge time series computed with the DYNPOUND method shown with the rated discharge time series and field measurements made at the Red River of the North at Fargo, North Dakota (U.S. Geological Survey station 05054000).

Discharge was computed for the time period between May 20 and July 10, 2019, to evaluate the DYNPOUND method at San Joaquin River near Mendota, California. Two field measurements are available for comparison during this time period. The DYNPOUND computed discharge is much higher than the observed and rated discharges at higher stage (figs. 36 and 37). Compared to the discharge observed on June 9, 2019, at 18:32 UTC, the DYNPOUND computed discharge is 32.3 percent higher. The MSLE for the computed discharge is 4.00×10^{-2} (table 15). The DYNPOUND method computation may be improved by implementing the feature to specify a stage/roughness relation for the cross section instead of specifying a Manning's *n* value for a subsection. Additionally, verifying accuracy of and correcting the representation of the cross-section geometry and discharge conditions within the rating may improve the results.

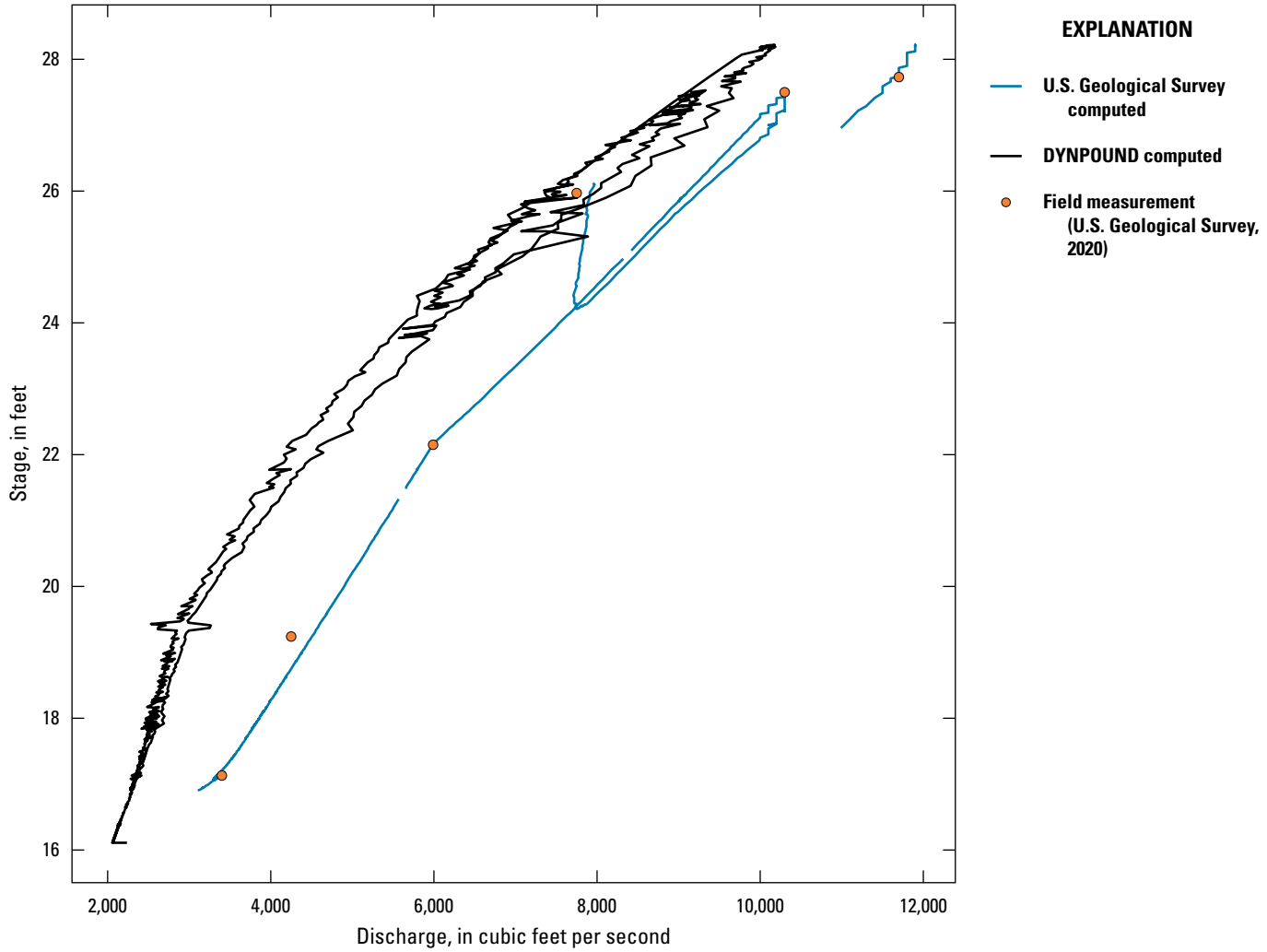

Figure 27. Stage/discharge relation of the discharge computed with the DYNPOUND method shown with U.S. Geological Survey-computed discharge and field measurements made at the Red River of the North at Fargo, North Dakota (U.S. Geological Survey station 05054000). Stage is referenced to 862.88 feet above North American Vertical Datum of 1988.

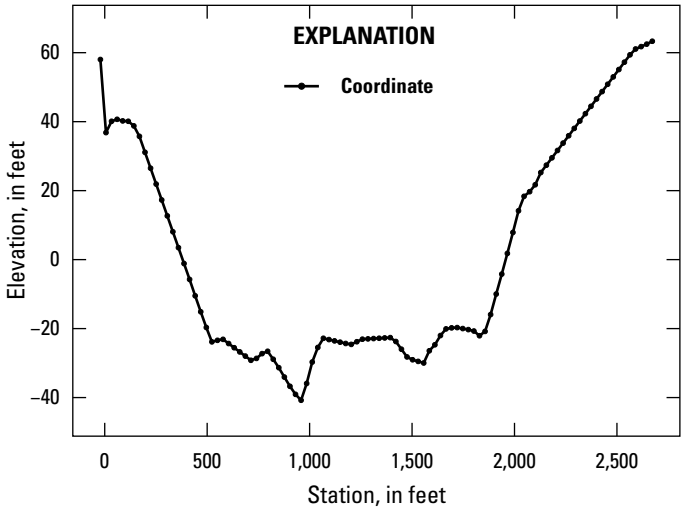

Figure 28. Cross section used in the computation of the discharge time series for the Mississippi River at St. Louis, Missouri (U.S. Geological Survey station 07010000). Elevation is referenced to 379.58 feet above North American Vertical Datum of 1988.

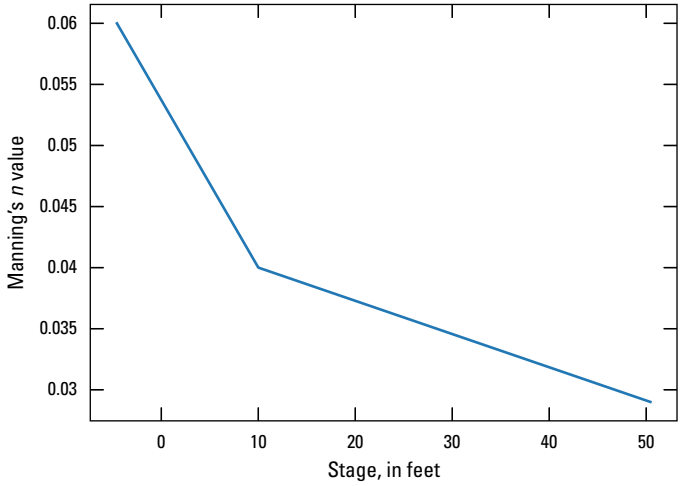

Figure 29. Relation between stage and roughness coefficient (Manning's *n*) used in the computation of discharge with the DYNMOD method for the Mississippi River at St. Louis, Missouri (U.S. Geological Survey station 07010000). Stage is referenced to 379.58 feet above North American Vertical Datum of 1988.

Table 10. Calibration results for the DYNMOD and DYNPOUND ratings at the Mississippi River at St. Louis, Missouri (U.S. Geological Survey station 07010000).

[Observed discharge data from U.S. Geological Survey (2020). MM, month; DD, day; YYYY, year; UTC, Universal Time Coordinated; ft^3/s, cubic feet per second; DYNMOD, the dynamic rating method that computes discharge from stage for compact channel geometry; SLE, squared logarithmic error; DYNPOUND, the newly developed method that solves for discharge in compact and compound channels; --, not applicable]

Measurement date (MM/DD/YYYY)	Measurement time (UTC)	Observed discharge (ft^3/s)	DYNMOD discharge (ft^3/s)	DYNMOD error (percent)	DYNMOD SLE	DYNPOUND discharge (ft^3/s)	DYNPOUND error (percent)	DYNPOUND SLE
10/31/2013	18:05	98,500	106,547	8.17	6.17×10^{-3}	123,851	25.7	5.25×10^{-2}
11/21/2013	17:57	106,000	105,171	−0.782	6.16×10^{-5}	122,172	15.3	2.02×10^{-2}
1/15/2014	19:24	99,100	95,117	4.02	1.68×10^{-3}	114,120	15.2	1.99×10^{-2}
2/20/2014	16:50	92,500	93,874	1.49	2.17×10^{-4}	114,548	23.8	4.57×10^{-2}
3/13/2014	16:34	167,000	172,994	3.59	1.24×10^{-3}	170,104	1.86	3.39×10^{-4}
4/10/2014	18:13	245,000	257,606	5.15	2.52×10^{-3}	226,891	−7.39	5.90×10^{-3}
5/21/2014	14:54	331,000	326,187	1.45	2.15×10^{-4}	276,064	−16.6	3.29×10^{-2}
6/5/2014	17:19	291,000	296,933	2.04	4.07×10^{-4}	257,341	−11.6	1.51×10^{-2}
7/10/2014	18:19	555,000	527,770	4.91	2.53×10^{-3}	412,971	−25.6	8.74×10^{-2}
8/14/2014	18:37	137,000	150,668	9.98	9.04×10^{-3}	154,331	12.7	1.42×10^{-2}
9/18/2014	15:09	400,000	403,045	0.761	5.75×10^{-5}	328,723	−17.8	3.85×10^{-2}
Mean	--	--	--	1.82	2.19×10^{-3}	--	1.42	3.02×10^{-2}

Dynamic Rating Application Recommendations

Through the course of developing and testing the dynamic rating method, the following are suggested best practices for using this method.

- Select an appropriate cross section for characterization of the channel geometry described as follows:
  - Select a reach where the flow is approximately one-dimensional (flow is orthogonal to the banks).
  - The flow direction should be well established in a one-dimensional nature. A rule of thumb for an ideal cross section would be one that is straight at least 100 times the bank full depth upstream and 100 times the bank full depth downstream.
  - Avoid cross sections within a river reach with abrupt changes in cross-sectional geometry.
- If possible, select multiple flood events to compute and assess the value of r in equation 9.
- Create the channel cross-section geometry properties and ensure that the stage/conveyance curve is smooth by subdividing the cross section.
- Choose a series of high-flow events to use as calibration for the Manning's roughness coefficient by the DYNMOD and DYNPOUND methods. Evaluate the methods using a different set of high-flow events.
- For compact channels (those without flood plains), although DYNPOUND was written for complex channels (those with flood plains), DYNPOUND may perform better than DYNMOD. As such, try both methods for all sites.

Table 11. Discharge computed for an event-based time series at the Mississippi River at St. Louis, Missouri (U.S. Geological Survey station 07010000) with the DYNMOD and DYNPOUND methods and the associated error.

[Observed discharge data from U.S. Geological Survey (2020). MM, month; DD, day; YYYY, year; UTC, Universal Time Coordinated; ft^3/s, cubic feet per second; DYNMOD, the dynamic rating method that computes discharge from stage for compact channel geometry; SLE, squared logarithmic error; DYNPOUND, the newly developed method that solves for discharge in compact and compound channels; --, not applicable]

Measurement date (MM/DD/YYYY)	Measurement time (UTC)	Observed discharge (ft^3/s)	DYNMOD discharge (ft^3/s)	DYNMOD error (percent)	DYNMOD SLE	DYNPOUND discharge (ft^3/s)	DYNPOUND error (percent)	DYNPOUND SLE
6/10/2015	15:29	513,000	521,007	1.56	2.40×10^{-4}	407,697	−20.5	5.28×10^{-2}
6/11/2015	15:09	490,000	506,108	3.29	1.05×10^{-3}	396,416	−19.1	4.49×10^{-2}
6/17/2015	22:52	576,000	579,642	0.632	3.97×10^{-5}	446,629	−22.5	6.47×10^{-2}
6/18/2015	23:06	605,000	604,613	−0.0639	4.09×10^{-7}	460,026	−24.0	7.50×10^{-2}
6/19/2015	17:09	633,000	648,606	2.47	5.93×10^{-4}	490,626	−22.5	6.49×10^{-2}
6/20/2015	16:19	672,000	662,168	−1.46	2.17×10^{-4}	493,240	−26.6	9.56×10^{-2}
6/21/2015	16:49	677,000	670,074	−1.02	1.06×10^{-4}	496,378	−26.7	9.63×10^{-2}
6/21/2015	17:12	670,000	667,185	−0.42	1.77×10^{-5}	492,984	−26.4	9.41×10^{-2}
6/21/2015	17:32	691,000	669,176	−3.16	1.03×10^{-3}	495,147	−28.3	1.11×10^{-1}
6/21/2015	17:48	693,000	670,667	−3.22	1.07×10^{-3}	496,766	−28.3	1.11×10^{-1}
6/21/2015	18:02	685,000	671,277	−2.00	4.10×10^{-4}	497,512	−27.4	1.02×10^{-1}
6/21/2015	18:15	696,000	667,850	−4.04	1.70×10^{-3}	494,296	−29.0	1.17×10^{-1}
6/21/2015	18:29	685,000	664,333	−3.02	9.39×10^{-4}	490,997	−28.3	1.11×10^{-1}
6/21/2015	18:43	688,000	660,654	−3.97	1.64×10^{-3}	487,546	−29.1	1.19×10^{-1}
6/21/2015	18:57	690,000	657,248	−4.75	2.36×10^{-3}	484,350	−29.8	1.25×10^{-1}
6/21/2015	19:10	691,000	658,895	−4.65	2.26×10^{-3}	486,067	−29.7	1.24×10^{-1}
6/21/2015	20:05	690,000	670,037	−2.89	8.62×10^{-4}	497,257	−27.9	1.07×10^{-1}
6/21/2015	20:18	687,000	668,785	−2.65	7.22×10^{-4}	495,843	−27.8	1.06×10^{-1}
6/21/2015	20:32	682,000	667,462	−2.13	4.64×10^{-4}	494,348	−27.5	1.04×10^{-1}
6/21/2015	20:46	690,000	666,155	−3.46	1.24×10^{-3}	492,872	−28.6	1.13×10^{-1}
6/21/2015	21:00	690,000	664,979	−3.63	1.36×10^{-3}	491,539	−28.8	1.15×10^{-1}
6/21/2015	21:13	689,000	666,017	−3.34	1.15×10^{-3}	492,603	−28.5	1.13×10^{-1}
6/21/2015	21:27	690,000	667,053	−3.33	1.14×10^{-3}	493,665	−28.5	1.12×10^{-1}
6/21/2015	22:47	686,000	655,874	−4.39	2.02×10^{-3}	483,251	−29.6	1.23×10^{-1}
6/21/2015	23:00	670,000	652,326	−2.64	7.15×10^{-4}	479,899	−28.4	1.11×10^{-1}
6/21/2015	23:14	664,000	653,527	−1.58	2.53×10^{-4}	481,333	−27.5	1.04×10^{-1}
6/21/2015	23:27	667,000	654,723	−1.84	3.45×10^{-4}	482,762	−27.6	1.05×10^{-1}
6/21/2015	23:43	668,000	656,184	−1.77	3.19×10^{-4}	484,505	−27.5	1.03×10^{-1}
6/22/2015	0:02	678,000	658,076	−2.94	8.90×10^{-4}	486,669	−28.2	1.10×10^{-1}
6/22/2015	0:18	668,000	660,762	−1.08	1.19×10^{-4}	489,298	−26.8	9.69×10^{-2}
6/22/2015	14:56	649,000	656,674	1.18	1.38×10^{-4}	487,324	−24.9	8.21×10^{-2}
6/23/2015	21:48	649,000	670,035	3.24	1.02×10^{-3}	499,177	−23.1	6.89×10^{-2}
6/24/2015	14:27	652,000	662,714	1.64	2.66×10^{-4}	491,487	−24.6	7.99×10^{-2}
6/27/2015	0:52	642,000	645,670	0.572	3.25×10^{-5}	481,318	−25.0	8.30×10^{-2}
6/27/2015	18:16	662,000	652,519	−1.43	2.08×10^{-4}	487,020	−26.4	9.42×10^{-2}
6/28/2015	21:13	700,000	672,513	−3.93	1.60×10^{-3}	498,927	−28.7	1.15×10^{-1}
7/1/2015	19:17	705,000	687,226	−2.52	6.52×10^{-4}	502,675	−28.7	1.14×10^{-1}
7/2/2015	18:04	642,000	675,390	5.20	2.57×10^{-3}	496,564	−22.7	6.60×10^{-2}
7/3/2015	17:40	647,000	671,405	3.77	1.37×10^{-3}	494,712	−23.5	7.20×10^{-2}

Table 11. Discharge computed for an event-based time series at the Mississippi River at St. Louis, Missouri (U.S. Geological Survey station 07010000) with the DYNMOD and DYNPOUND methods and the associated error.—Continued

[Observed discharge data from U.S. Geological Survey (2020). MM, month; DD, day; YYYY, year; UTC, Universal Time Coordinated; ft^3/s, cubic feet per second; DYNMOD, the dynamic rating method that computes discharge from stage for compact channel geometry; SLE, squared logarithmic error; DYNPOUND, the newly developed method that solves for discharge in compact and compound channels; --, not applicable]

Measurement date (MM/DD/YYYY)	Measurement time (UTC)	Observed discharge (ft^3/s)	DYNMOD discharge (ft^3/s)	DYNMOD error (percent)	DYNMOD SLE	DYNPOUND discharge (ft^3/s)	DYNPOUND error (percent)	DYNPOUND SLE
7/4/2015	23:57	632,000	660,803	4.56	1.99×10^{-3}	488,807	−22.7	6.60×10^{-2}
7/5/2015	15:22	623,000	650,799	4.46	1.91×10^{-3}	483,875	−22.3	6.39×10^{-2}
7/7/2015	16:07	555,000	581,397	4.76	2.16×10^{-3}	442,827	−20.2	5.10×10^{-2}
7/7/2015	19:37	542,000	572,602	5.65	3.02×10^{-3}	436,160	−19.5	4.72×10^{-2}
7/8/2015	16:07	500,000	550,114	10.0	9.12×10^{-3}	425,120	−15.0	2.63×10^{-2}
7/9/2015	15:44	529,000	561,777	6.20	3.61×10^{-3}	434,365	−17.9	3.88×10^{-2}
7/10/2015	14:47	583,000	609,643	4.57	2.00×10^{-3}	463,880	−20.4	5.22×10^{-2}
7/11/2015	15:47	631,000	639,584	1.36	1.83×10^{-4}	480,126	−23.9	7.47×10^{-2}
7/12/2015	23:45	592,000	607,837	2.68	6.97×10^{-4}	457,480	−22.7	6.64×10^{-2}
7/13/2015	19:15	567,000	598,859	5.62	2.99×10^{-3}	455,084	−19.7	4.83×10^{-2}
7/14/2015	15:14	565,000	593,089	4.97	2.35×10^{-3}	450,621	−20.2	5.12×10^{-2}
7/15/2015	14:34	550,000	603,343	9.70	8.57×10^{-3}	458,817	−16.6	3.29×10^{-2}
7/16/2015	14:08	561,000	587,649	4.75	2.15×10^{-3}	446,697	−20.4	5.19×10^{-2}
7/17/2015	14:30	509,000	543,720	6.82	4.35×10^{-3}	417,243	−18.0	3.95×10^{-2}
7/18/2015	16:31	467,000	506,263	8.41	6.52×10^{-3}	396,197	−15.2	2.70×10^{-2}
7/19/2015	16:31	467,000	497,223	6.47	3.93×10^{-3}	392,552	−15.9	3.02×10^{-2}
7/21/2015	19:36	537,000	555,475	3.44	1.14×10^{-3}	428,400	−20.2	5.10×10^{-2}
7/24/2015	15:48	500,000	533,626	6.73	4.24×10^{-3}	413,031	−17.4	3.65×10^{-2}
7/25/2015	15:21	454,000	494,058	8.82	7.15×10^{-3}	387,429	−14.7	2.51×10^{-2}
7/26/2015	15:25	412,000	450,730	9.40	8.07×10^{-3}	360,010	−12.6	1.82×10^{-2}
7/27/2015	14:24	412,000	447,976	8.73	7.01×10^{-3}	361,637	−12.2	1.70×10^{-2}
7/28/2015	14:14	422,000	452,366	7.20	4.83×10^{-3}	363,577	−13.8	2.22×10^{-2}
7/29/2015	13:53	428,000	453,158	5.88	3.26×10^{-3}	363,829	−15.0	2.64×10^{-2}
7/31/2015	18:33	407,000	443,599	8.99	7.41×10^{-3}	357,040	−12.3	1.72×10^{-2}
8/3/2015	18:11	375,000	401,511	7.07	4.67×10^{-3}	329,327	−12.2	1.69×10^{-2}
8/5/2015	17:14	346,000	369,670	6.84	4.38×10^{-3}	307,679	−11.1	1.38×10^{-2}
8/6/2015	15:09	320,000	365,868	14.3	1.79×10^{-2}	305,039	−4.68	2.29×10^{-3}
8/7/2015	16:36	318,000	336,926	5.95	3.34×10^{-3}	284,208	−10.6	1.26×10^{-2}
8/11/2015	17:21	233,000	273,525	17.4	2.57×10^{-2}	239,576	2.82	7.75×10^{-4}
Mean	--	--	--	2.18	2.76×10^{-3}	--	−22.1	7.11×10^{-2}

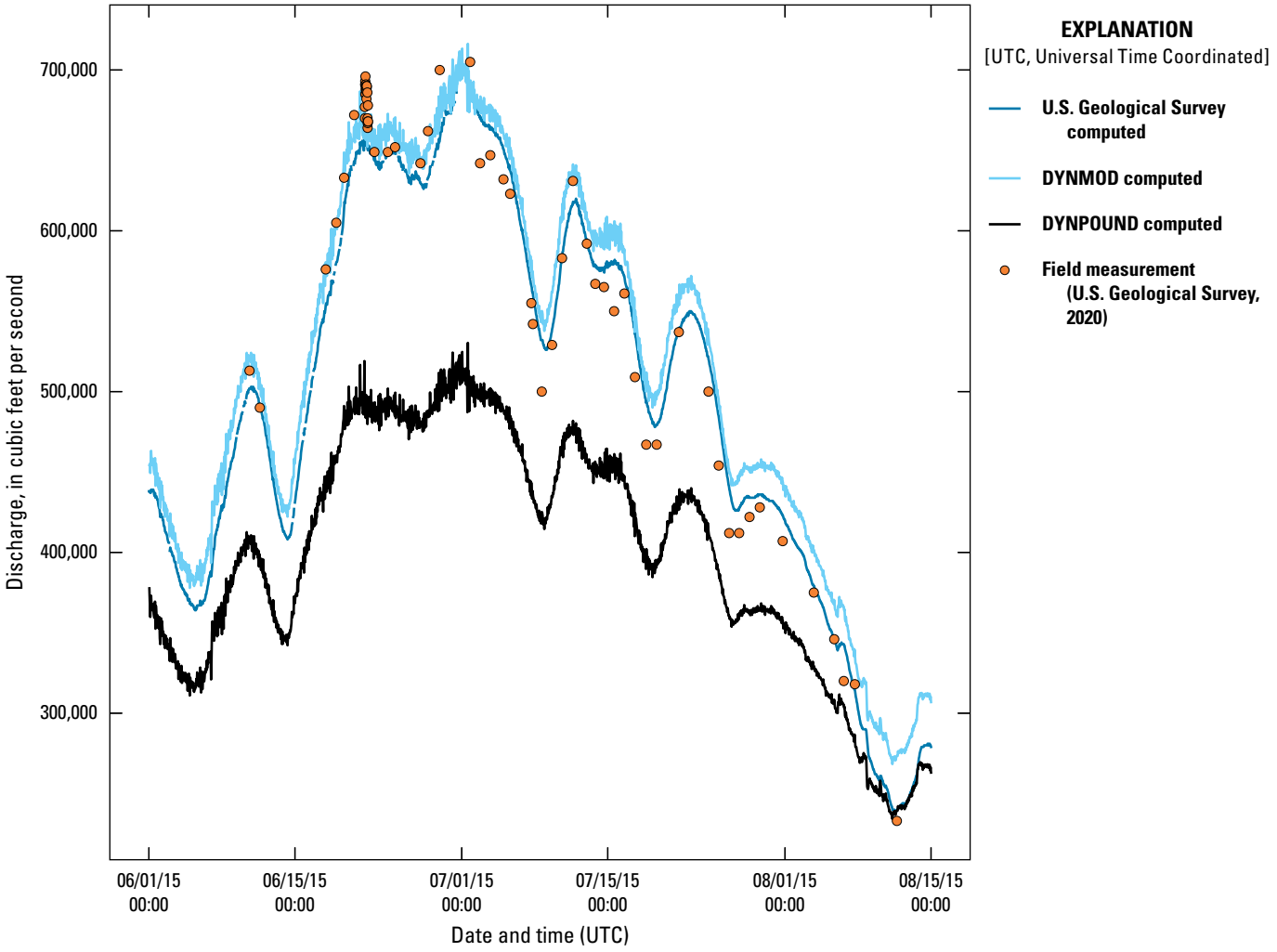

Figure 30. Discharge time series computed with the DYNMOD and DYNPOUND methods shown with the U.S. Geological Survey-computed discharge time series and field measurements made at the Mississippi River at St. Louis, Missouri (U.S. Geological Survey station 07010000).

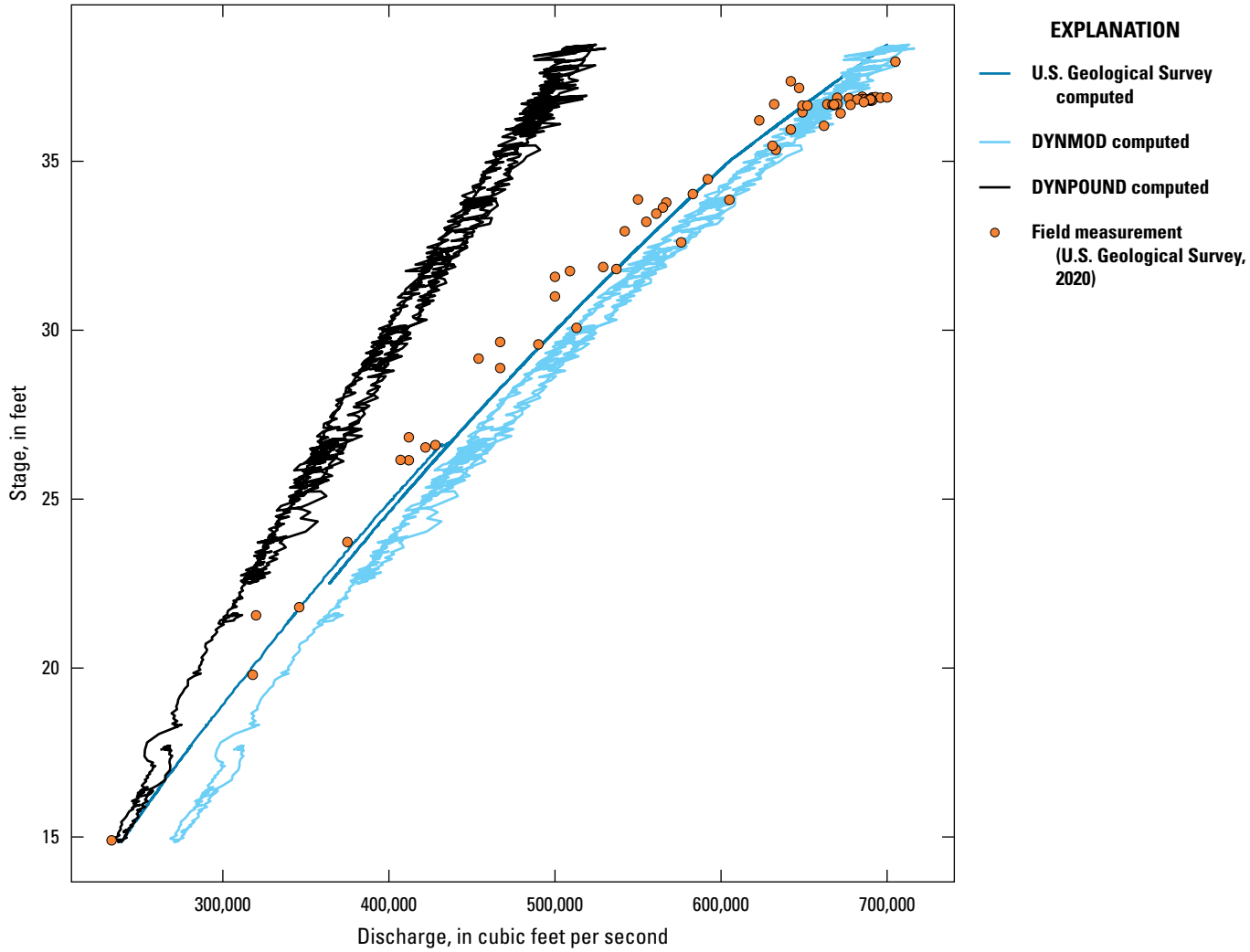

Figure 31. Stage/discharge relation of the discharge computed with the DYNMOD and DYNPOUND methods shown with U.S. Geological Survey-computed discharge and field measurements made at the Mississippi River at St. Louis, Missouri (U.S. Geological Survey station 07010000). Stage is referenced to 379.58 feet above North American Vertical Datum of 1988.

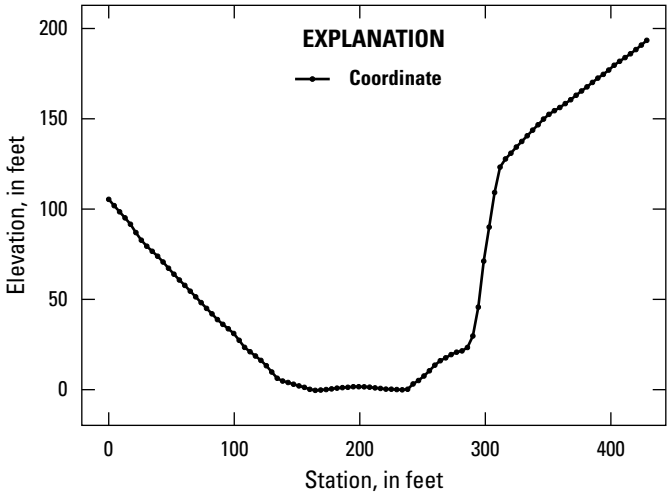

Figure 32. Cross section used in the computation of the discharge time series for the Rio Grande near Cerro, New Mexico (U.S. Geological Survey station 08263500). Elevation is referenced to 7,110 feet above National Geodetic Vertical Datum of 1929.

Table 12. Calibration results for the DYNMOD and DYNPOUND ratings at the Rio Grande Near Cerro, New Mexico (U.S. Geological Survey station 08263500).

[Observed discharge data from U.S. Geological Survey (2020). MM, month; DD, day; YYYY, year; UTC, Universal Time Coordinated; ft^3/s, cubic feet per second; DYNMOD, the dynamic rating method that computes discharge from stage for compact channel geometry; SLE, squared logarithmic error; DYNPOUND, the newly developed method that solves for discharge in compact and compound channels; --, not applicable]

Measurement date (MM/DD/YYYY)	Measurement time (UTC)	Observed discharge (ft^3/s)	DYNMOD discharge (ft^3/s)	DYNMOD error (percent)	DYNMOD SLE	DYNPOUND discharge (ft^3/s)	DYNPOUND error (percent)	DYNPOUND SLE
10/9/2014	15:02	306	299	−2.05	5.36×10^{-4}	296	−2.99	1.10×10^{-3}
12/4/2014	17:25	451	465	3.29	9.35×10^{-4}	460	2.19	3.90×10^{-4}
1/26/2015	17:16	273	274	0.381	1.34×10^{-5}	271	−0.558	5.41×10^{-5}
2/26/2015	16:16	349	353	1.15	1.30×10^{-4}	349	0	0
4/14/2015	17:59	189	166	−11.7	1.68×10^{-2}	165	−12.4	1.84×10^{-2}
7/30/2015	16:18	381	408	7.11	4.69×10^{-3}	403	6.00	3.15×10^{-3}
8/20/2015	14:50	167	135	−18.8	4.52×10^{-2}	134	−19.4	4.85×10^{-2}
Mean	--	--	--	−2.95	9.77×10^{-3}	--	−3.86	1.02×10^{-2}

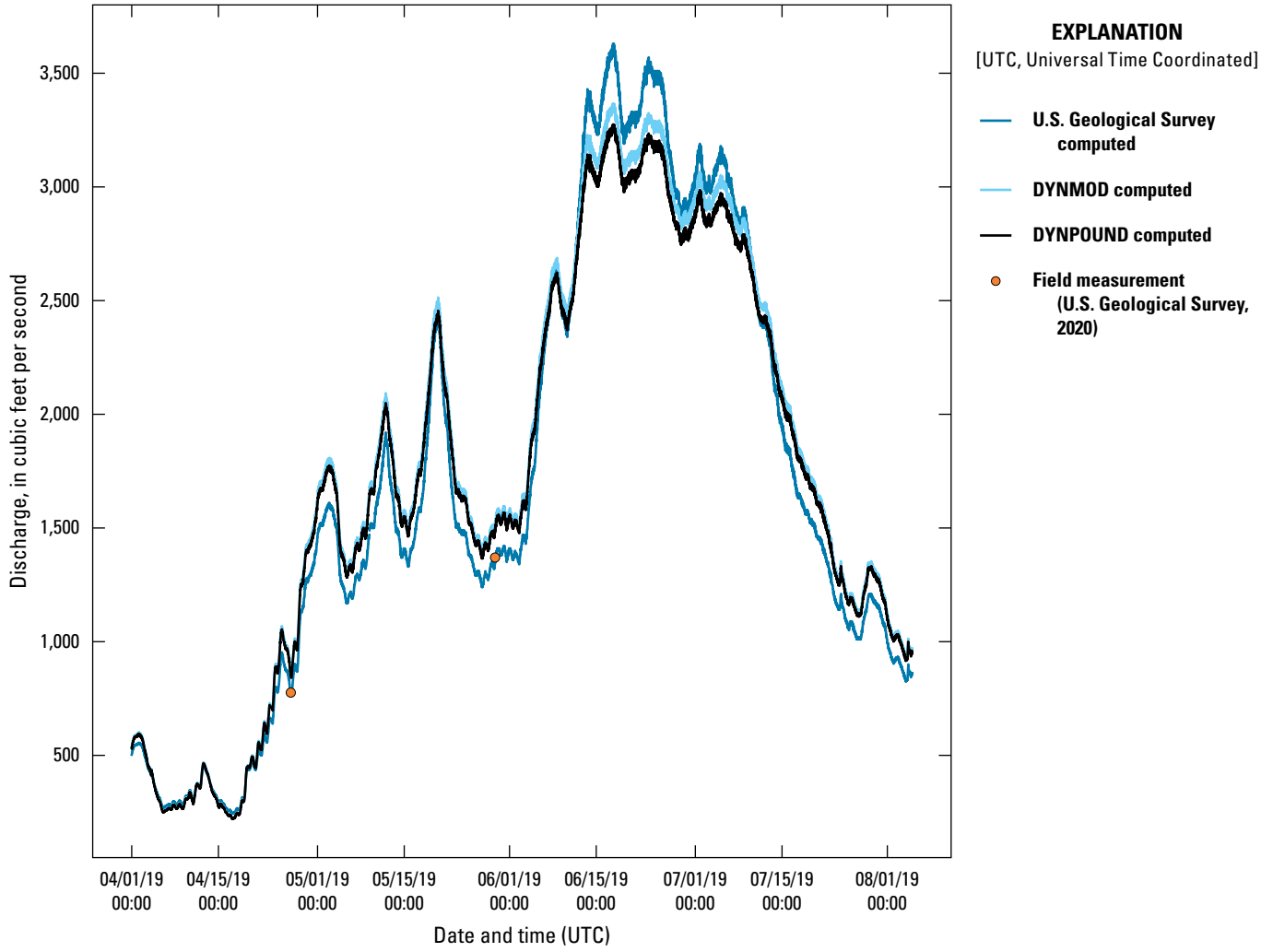

Figure 33. Discharge time series computed with the DYNMOD and DYNPOUND methods shown with the U.S. Geological Survey-computed discharge time series and field measurements made at the Rio Grande near Cerro, New Mexico (U.S. Geological Survey station 08263500).

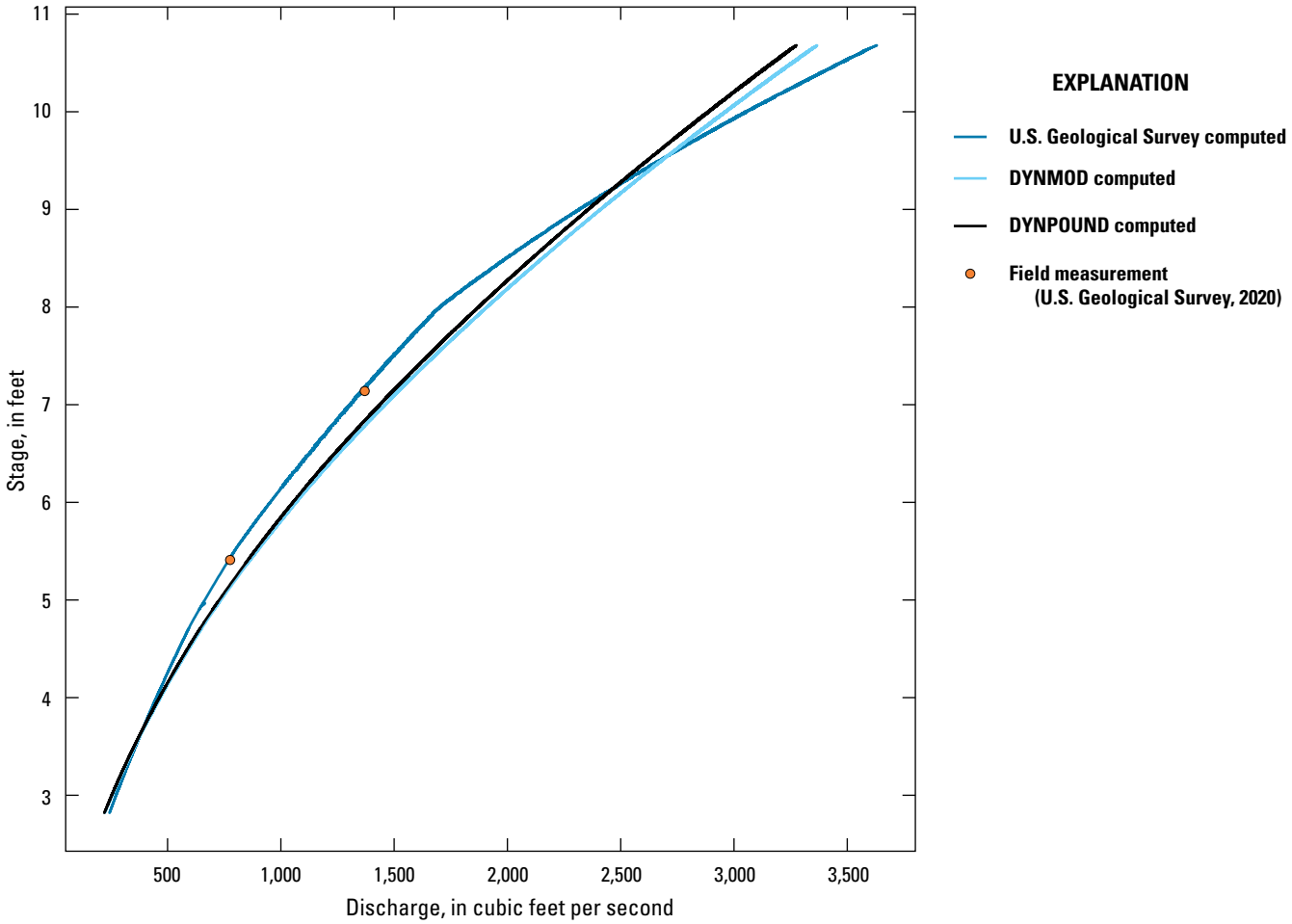

Figure 34. Stage/discharge relation of the discharge computed with the DYNMOD and DYNPOUND methods shown with U.S. Geological Survey-computed discharge and field measurements made at Rio Grande near Cerro, New Mexico (U.S. Geological Survey station 08263500). Elevation is referenced to 7,110 feet above National Geodetic Vertical Datum of 1929.

Table 13. Discharge computed with the DYNMOD and DYNPOUND methods and associated error for an event-based time series at the Rio Grande near Cerro, New Mexico (U.S. Geological Survey station 08263500).

[Observed discharge data from U.S. Geological Survey (2020). MM, month; DD, day; YYYY, year; UTC, Universal Time Coordinated; ft^3/s, cubic feet per second; DYNMOD, the dynamic rating method that computes discharge from stage for compact channel geometry; SLE, squared logarithmic error; DYNPOUND, the newly developed method that solves for discharge in compact and compound channels; --, not applicable]

Measurement date (MM/DD/YYYY)	Measurement time (UTC)	Observed discharge (ft^3/s)	DYNMOD discharge (ft^3/s)	DYNMOD error (percent)	DYNMOD SLE	DYNPOUND discharge (ft^3/s)	DYNPOUND error (percent)	DYNPOUND SLE
4/26/2019	16:20	776	861	11.0	1.08×10^{-2}	850	9.62	8.30×10^{-3}
5/29/2019	16:00	1,370	1,521	11.1	1.09×10^{-2}	1,495	9.18	7.62×10^{-3}
Mean	--	--	--	11.05	1.09×10^{-2}	--	9.40	7.96×10^{-3}

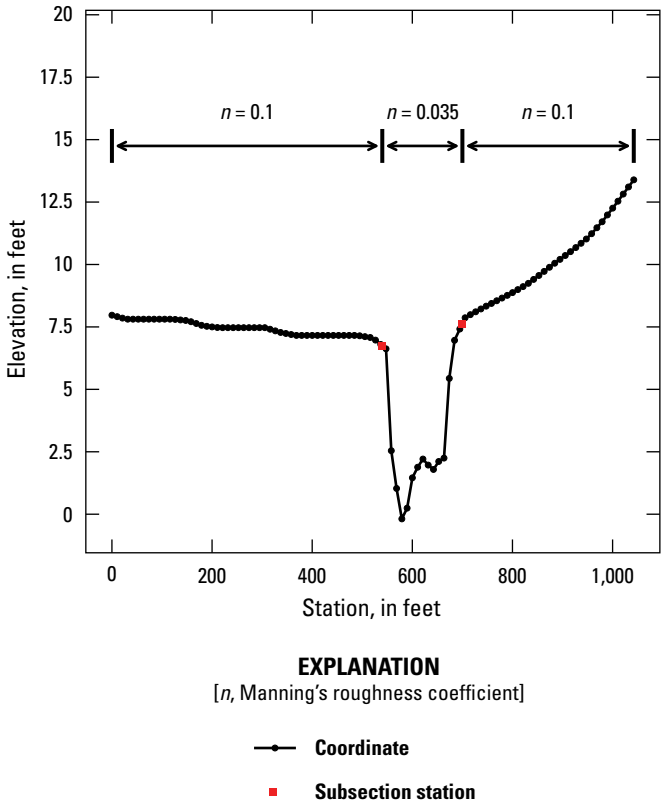

Figure 35. Cross section used in the computation of the discharge time series for the San Joaquin River Near Mendota, California (U.S. Geological Survey station 11254000). Elevation is referenced to 133.35 feet above North American Vertical Datum of 1988.

Table 14. Calibration results for the DYNPOUND rating at the San Joaquin River near Mendota, California (U.S. Geological Survey station 11254000).

[Observed discharge data from U.S. Geological Survey (2020). MM, month; DD, day; YYYY, year; UTC, Universal Time Coordinated; ft^3/s, cubic feet per second; SLE, squared logarithmic error; DYNPOUND, the newly developed method that solves for discharge in compact and compound channels; --, not applicable]

Measurement date (MM/DD/YYYY)	Measurement time (UTC)	Observed discharge (ft^3/s)	DYNPOUND discharge (ft^3/s)	DYNPOUND error (percent)	DYNPOUND SLE
10/6/2016	15:49	347	350	0.989	7.41×10^{-5}
12/1/2016	17:22	22	34	58.4	1.90×10^{-1}
1/10/2017	20:48	0.67	17	2,530	1.05×10^{1}
1/26/2017	0:21	767	783	2.19	4.26×10^{-4}
2/22/2017	22:45	3,840	6,362	65.7	2.55×10^{-1}
4/4/2017	16:40	3,320	5,354	61.3	2.28×10^{-1}
5/26/2017	17:58	273	359	31.7	7.50×10^{-2}
7/21/2017	15:05	567	621	9.62	8.28×10^{-3}
9/21/2017	22:51	421	434	3.27	9.25×10^{-4}
Mean	--	--	--	307	1.25

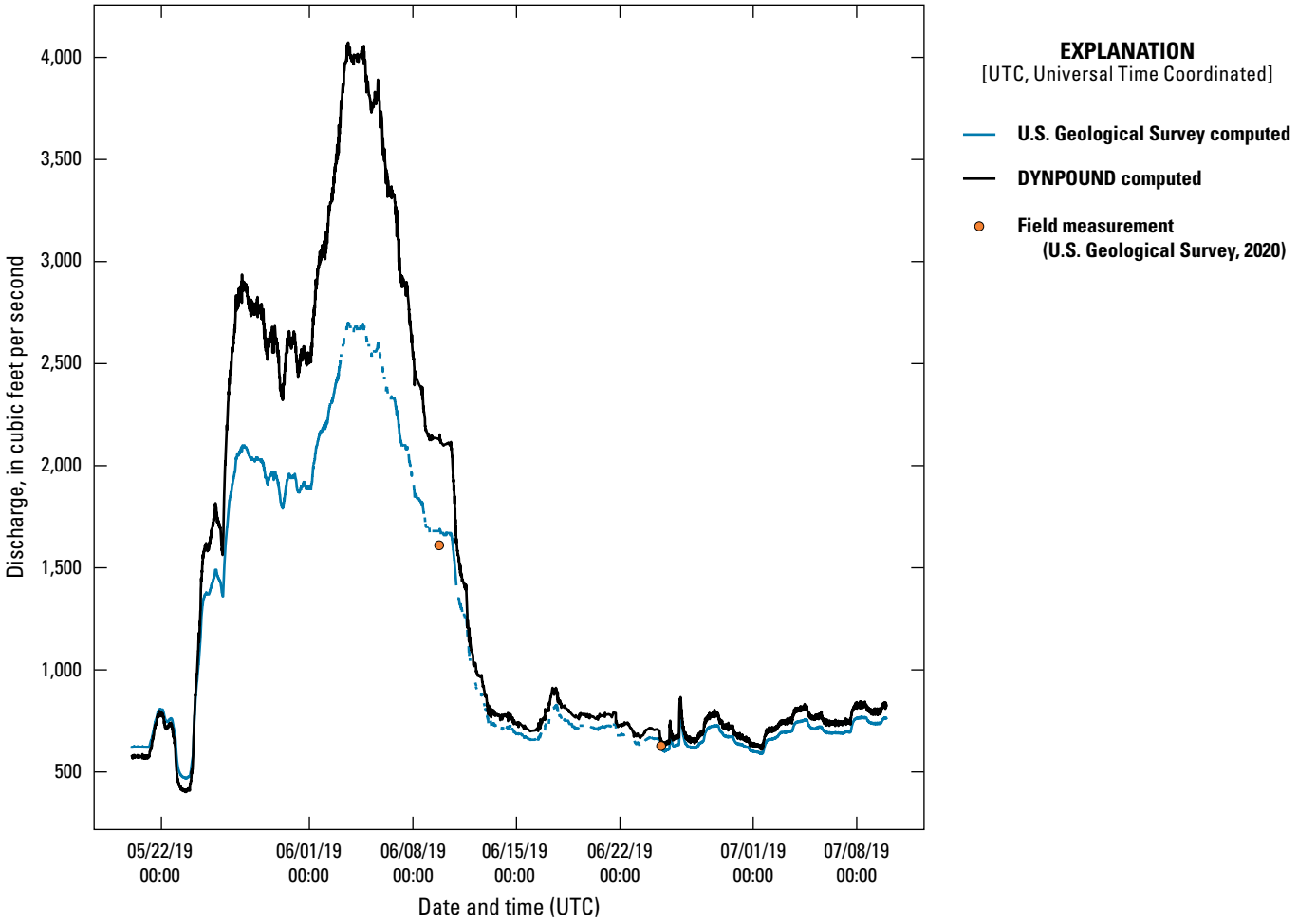

Figure 36. Discharge time series computed with the DYNPOUND method shown with the U.S. Geological Survey-computed time series and field measurements made at the San Joaquin River near Mendota, California (U.S. Geological Survey station 11254000).

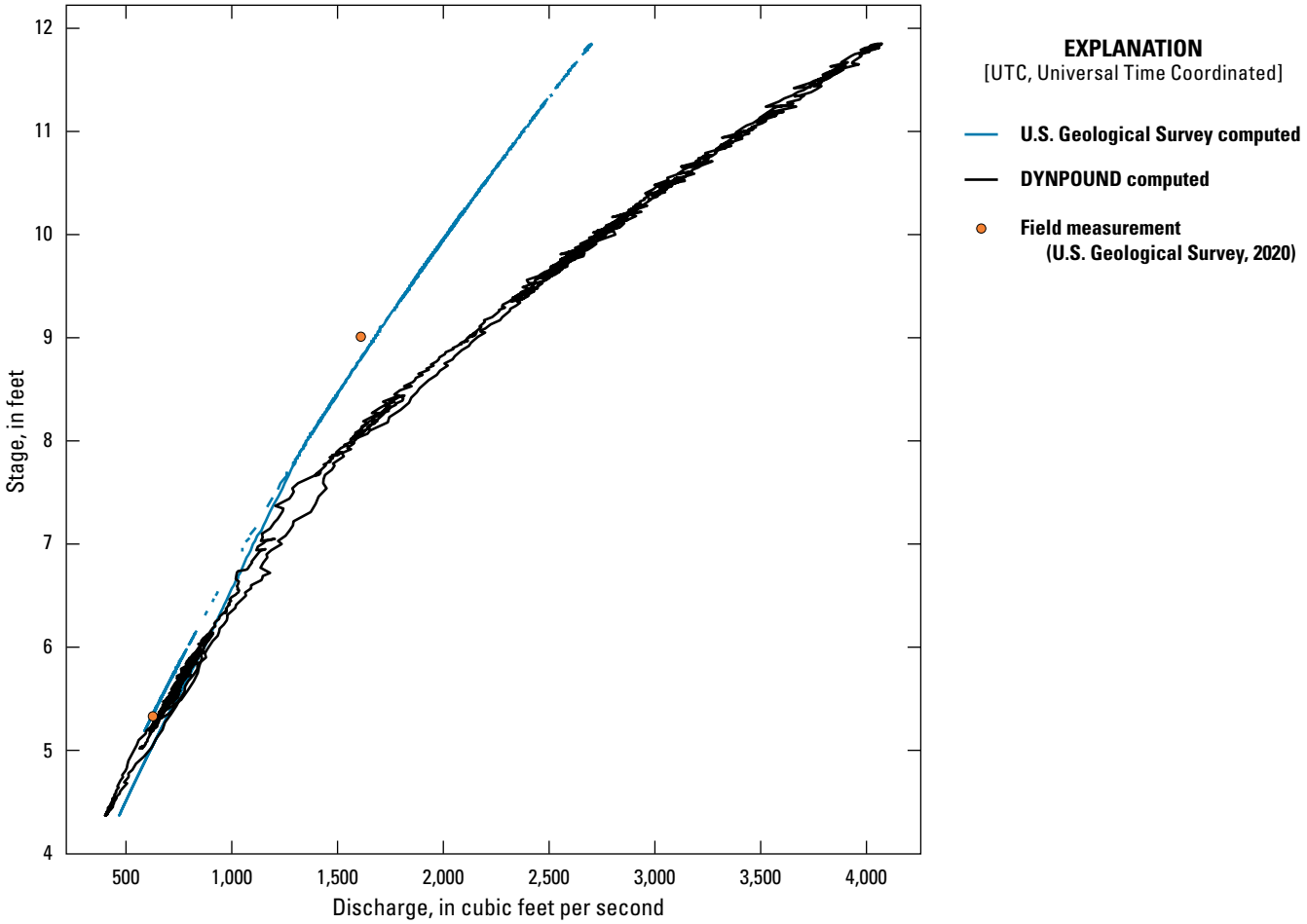

Figure 37. Stage/discharge relation of the discharge computed with the DYNPOUND method shown with U.S. Geological Survey-computed discharge and field measurements made at the San Joaquin River near Mendota, California (U.S. Geological Survey station 11254000). Stage is referenced to 133.35 feet above North American Vertical Datum of 1988.

Table 15. Discharge computed with the DYNPOUND method and associated error for an event-based time series at San Joaquin River near Mendota, California (U.S. Geological Survey station 11254000).

[Observed discharge data from U.S. Geological Survey (2020); MM, month; DD, day; YYYY, year; UTC, Universal Time Coordinated; ft^3/s, cubic feet per second; DYNPOUND, the newly developed method that solves for discharge in compact and compound channels; SLE, squared logarithmic error; --, not applicable]

Measurement date (MM/DD/YYYY)	Measurement time (UTC)	Observed discharge (ft^3/s)	DYNPOUND discharge (ft^3/s)	DYNPOUND error (percent)	DYNPOUND SLE
6/9/2019	18:32	1,610	2,129	32.3	7.81×10^{-2}
6/24/2019	18:40	627	655	4.50	1.91×10^{-3}
Mean	--	--	--	18.4	4.00×10^{-2}

Summary

Ratings are used for a variety of reasons in water-resources investigations, but a predominant use of ratings is at streamgages, where autonomously collected stage is converted to discharge by use of a rating. In the absence of direct discrete continuous discharge measurements, discharge typically is determined through surrogate measures of one or more variables such as stage, water-surface slope, rate of change in stage, or index velocity collected at a streamgage. The rating is developed and calibrated using discharge measurements collected onsite by field staff. The simplest rating relates discharge to stage of the river (simple rating). Hydrologists and engineers have long recognized hysteresis (loops) exist in relations between stage and discharge. The hysteresis is sometimes small enough that it is hidden within the error of the measurements. Likewise, when the time of reporting of the discharge is large enough, the hysteresis averages out. For some sites, simple ratings work well. Simple ratings do not work as well for streamgages on low-gradient streams, streams with variable backwater, streams with large amounts of channel or overbank storage, streams with highly unsteady flow, or streams with highly mobile beds. In these cases, a complex rating is often needed. A complex rating relates discharge to stage and other variables because of the lack of a unique, univariate relation between stage and discharge. A dynamic rating is a rating that accounts for a variable energy slope owing to unsteady flow accelerations.

A previously developed dynamic rating method (DYNMOD) to compute discharge from a stage time series, which was developed for compact channel geometry, was described. A new dynamic rating method (DYNPOUND), which has been developed for compact and compound channel geometry, was introduced in this report. The mathematical formulation for DYNPOUND was derived and a numerical solution method was then formulated and described.

Discharge time series computed with the DYNMOD and DYNPOUND rating methods were compared to results computed from the one-dimensional unsteady shallow water equations. The simulated discharge time series, and corresponding simulated stage time series, were generated using one-dimensional hydraulic modeling software. The time series were simulated using a prismatic channel created from a compound cross section. Four scenarios were created using two different bed slopes and four different hydrographs that serve as the upstream boundary conditions. The hydrographs were created to capture a range of unsteadiness in the flow conditions. In the comparison, the discharge computed with the DYNPOUND method had a lower mean squared logarithmic error (MSLE) than discharge computed with the DYNMOD method in all scenarios. The MSLE for the DYNPOUND computed discharge ranges from 2.51×10^{-7} to 1.91×10^{-4}, and the MSLE computed from the DYNMOD computed discharge ranges from 2.75×10^{-2} to 3.40×10^{-2}. In all cases, the DYNPOUND method outperformed the DYNMOD method.

The results computed with the dynamic rating methods were then compared to field data previously collected at U.S. Geological Survey streamgage sites. Six streamgage sites were chosen for comparison. Cross-section geometry for the streamgage sites was created by combining "station, elevation" coordinates from acoustic doppler current profiler discharge measurements with digital elevation data. Coordinate data were extracted from previously collected discharge measurements. Bed slopes for the sites were estimated from topographic maps. Continuous stage, needed to compute discharge with the dynamic rating methods, were obtained from the U.S. Geological Survey National Water Information System database. Field measurements, which were used to calibrate and evaluate the performance of the dynamic rating methods, were also obtained from the National Water Information System database, along with discharge time series, which were computed with more traditional simple rating methods.

Dynamic ratings were developed and calibrated for each site. Calibration was accomplished by adjusting n values and adding subsections to the cross section to minimize the MSLE with respect to field measurements for the respective site. DYNMOD failed to compute discharge for the entire calibration time period at 3 of the 6 sites. DYNPOUND successfully computed discharge for the entire calibration time series at each site. For the three sites that the DYNMOD method successfully computed the entire time series, MSLE had a range of 2.19×10^{-3} to 9.77×10^{-3}, and the DYNPOUND calibration has a range of 3.7×10^{-3} to 1.25.

One event-based time period was chosen for each site to evaluate the calibration of the dynamic rating methods. For each dynamic rating method, the calibrated rating was used, along with the stage time series from the time period, to compute a discharge time series. The DYNMOD method was not used to compute discharge for sites at which the method failed to compute the full calibration time period. The range of MSLE for the DYNMOD time series is 2.73×10^{-3} to 3.14×10^{-2}, and the range of MSLE for the DYNPOUND method is 3.64×10^{-3} to 7.23×10^{-2}. For sites that DYNMOD successfully computed the full calibration time series, DYNMOD performs better than DYNPOUND when using MSLE as a performance metric. However, DYNMOD failed to compute calibration time series at 3 out of 6 field sites, which indicates DYNPOUND is a more robust method. Additionally, improvements, including variable roughness with stage, can be made to the implementation of the DYNPOUND method, which may improve the computed results.

Acknowledgments

The field offices of the California Water Science Center, Caribbean-Florida Water Science Center, Central Midwest Water Science Center, Dakota Water Science Center, Lower Mississippi-Gulf Water Science Center, Nebraska Water Science Center, New England Water Science Center, New

Mexico Water Science Center, Ohio-Kentucky-Indiana Water Science Center, Oregon Water Science Center, Upper Midwest Water Science Center, Utah Water Science Center, Virginia and West Virginia Water Science Center, and Washington Water Science Center were instrumental in providing site data for this project.

References Cited

Corbett, D.M., 1943, Stream-gaging procedure: U.S. Geological Survey Water-Supply Paper 888, 153 p. [Also available at https://doi.org/10.3133/wsp888.]

Cunge, J.A., Holly, F.M., and Verwey, A., 1980, Practical aspects of computational river hydraulics: Marshfield, Mass., Pittman Publishing, 420 p.

Dahlquist, G., and Björck, Å., 1974, Numerical methods: Englewood Cliffs, N.J., Prentice-Hall, 573 p.

Davidian, J., 1984, Computation of water-surface profiles in open channels: U.S. Geological Survey Techniques of Water-Resources Investigations, book 3, chap. A15, 48 p. [Also available at https://doi.org/10.3133/twri03A15.]

Domanski, M.M., Holmes, R.R., and Heal, E.N., 2022a, Dynamic rating method for computing discharge from time series stage data—Site datasets: U.S. Geological Survey data release, https://doi.org/10.5066/P955QRPQ.

Domanski, M.M., Holmes, R.R., and Heal, E.N., 2022b, Dynamic stage to discharge rating model archive: U.S. Geological Survey data release, https://doi.org/10.5066/P9YUV9DG.

Esri, 2021, ArcGIS Pro: Esri website, accessed March 2020 at https://www.esri.com/en-us/arcgis/products/arcgis-pro/overview.

Faye, R.E., and Cherry, R.N., 1980, Channel and dynamic flow characteristics of the Chattahoochee River, Buford Dam to Georgia Highway 141: U.S. Geological Survey Water-Supply Paper 2063, 66 p. [Also available at https://doi.org/10.3133/wsp2063.]

Fread, D.L., 1973, A dynamic model of stage-discharge relations affected by changing discharge: Silver Spring, Md., National Oceanic and Atmospheric Administration, National Weather Service, Office of Hydrology, 1638 p.

Fread, D.L., 1975, Computation of stage-discharge relationships affected by unsteady flow: Journal of the American Water Resources Association, v. 11, no. 2, p. 213–228. [Also available at https://doi.org/10.1111/j.1752-1688.1975.tb00674.x.]

French, R.H., 1985, Open channel hydraulics: New York, McGraw-Hill Book Company, 705 p.

Henderson, F.M., 1966, Open channel flow: New York, The Macmillan Company, 522 p.

Holmes, R.R., Jr., 2017, Streamflow ratings, chap. 6 *of* Singh, V.P., ed., Handbook of applied hydrology (2d ed.): New York, McGraw-Hill Book Company, p. 6-1–6-14.

Jones, B.E., 1915, A method of correcting river discharge for a changing stage: U.S. Geological Survey Water-Supply Paper 375–E, 130 p. [Also available at https://doi.org/10.3133/wsp375E.]

Michigan State University, 2020, Michigan State University map library: accessed March 2020 at https://msugis.maps.arcgis.com/home/index.html.

Rantz, S.E., and others, 1982, Measurement and computation of streamflow—Volume 2. Computation of discharge: U.S. Geological Survey Water-Supply Paper 2175, 631 p. [Also available at https://pubs.usgs.gov/wsp/wsp2175/wsp2175_vol2.pdf.]

U.S. Army Corps of Engineers, 2016, Hydrologic engineering center river analysis system HEC-RAS 5.0 user's manual: Davis, Calif., Hydrologic Engineering Center, 960 p. [Also available at https://www.hec.usace.army.mil/software/hec-ras/documentation/HEC-RAS%205.0%20Users%20Manual.pdf.]

U.S. Department of Agriculture, 2021, Geospatial Data Gateway: accessed March 2020 at https://datagateway.nrcs.usda.gov/GDGHome.aspx.

U.S. Geological Survey, 2015, AreaComp2, version 2-1.04: U.S. Geological Survey website, accessed March 2020 at https://hydroacoustics.usgs.gov/indexvelocity/AreaComp.shtml.

U.S. Geological Survey, 2017, U.S. Geological Survey TNM Hydrography (National Hydrography Dataset): accessed March 2021 at https://apps.nationalmap.gov/downloader/#/.

U.S. Geological Survey, 2020, USGS water data for the Nation: U.S. Geological Survey National Water Information System database, accessed March 2020 at https://doi.org/10.5066/F7P55KJN.

For more information about this publication, contact
Director, USGS Central Midwest Water Science Center
405 North Goodwin
Urbana, IL 61801
217–328–8747
For additional information, visit
https://www.usgs.gov/centers/cm-water
Publishing support provided by the
Rolla and Lafayette Publishing Service Centers

ISSN 2331-1258 (online)
https://doi.org/10.3133/ofr20221031